CDF/DOC/CALORIMETRY/CDFR/6245
January 10, 2003
V 1

Testing Multi-Anode PMTs for CPR2

Kouji Sato[1], Hiroshi Kaneko, Shin Yamauchi, Ai Nagano, F. Ukegawa, S. Kim

Institute of Physics, University of Tsukuba
Tsukuba-shi, Ibaraki-ken 305-8571, Japan

Abstract

We have tested Hamamatsu H6568 16-pixel multi-anode photomultiplier tubes that have been considered for the Run-IIb CPR detector. We characterize tubes in terms of anode uniformity, gain, cross-talk, linearity and others. We find an anode uniformity of about 10%, which is much better than that advertised by Hamamatsu, provided that we use the tube the way we would for CPR2. Clear single-photoelectron peaks are observed, and thus we should have no difficulties in measuring 10-photoelectron minimum ionizing particles expected in CPR2. Linearity measurements indicate that a linear base is probably not adequate and we need a tapered base. Estimates of absolute gains using single photoelectron peaks are not straightforward because of the saturations, but measurements of tubes with tapered base give a good agreement with Hamamatsu data sheet.

1 Introduction

The CPR detector for the Run-IIb CDF experiment will be a scintillating tile/fiber detector [1] similar to the upgraded end-plug calorimeter (PEM) and its preshower counter (PPR). Light produced in scintillating tiles will be collected and converted to a longer wavelength (green light) by the wavelength-shifting fiber (Kuraray Y-11) imbedded in the groove in the tile. The green light will be transmitted through a clear fiber to photomultiplier tubes (PMTs). The current choice is to use a multi-anode PMT so as to save the tube count and cost.

A candidate is Hamamatsu H6568, which has 16 anode channels with an approximate pixel size of 4 mm $\times$ 4 mm. H6568 is the name for a tube-base assembly, and the bare tube is R5900-00-M16. A mechanical drawing from Hamamatsu is reproduced in Figure 1. It has a normal photocathode, sensitive mainly to blue light, and 12-stage metal-channel dynodes and a 16-channel anode. Model H6568MOD has a DY12 output as well. The high voltage bleeder circuit for H6568 has equal voltage division ("linear" base) among all multiplication stages (Figure 2). A typical gain at -800 V is 3.3×10^6. Note that the cathode and the dynodes are electrically common to all 16 channels and only the anode has the individual (pixel) structure.

We have purchased ten tubes each from the H6568 and H6568MOD models, and five tubes from each model have been sent to our colleagues in the US for evaluation [2]. The rest are kept

[1] 佐藤幸司. No relation to Koji "doraemon@fnal.gov" Sato (佐藤構二).

and tested at Tsukuba. The data sheet from Hamamatsu is listed as Tables 1 and 2. The gain can be calculated from the cathode and anode sensitivities. In case you cannot read Japanese, Sk stands for the cathode sensitivity and Sp the anode sensitivity. You will find that the gains are on the high side.

We want to test the tubes and determine their characteristics so as to demonstrate that they are suited for our planned use in CPR2. To be more specific, we want to examine if (a) the tube has a sensitivity to the expected MIP signal (5 to 10 photoelectrons) with good resolution, (b) the response variation among 16 pixels within a tube is small enough, (c) the cross-talk among anode pixels, which is inevitable by tube construction, is small enough, and (d) the linearity is good enough for larger pulses expected from high energy electrons. Also, we had wanted to check its timing characteristics with the dynode signal, although it now has less interest because the CEM timing project is under way. Below we describe some of the measurements we have performed related to these issues.

Before proceeding, we give the definition of the channels. If you look at the tube into the cathode (front view), top-right is Channel 1, top-left is 4, and bottom-left is 16 (Figure 3). They are engraved in the piece of metal near the tube surface.

We also define x and y axes as the horizontal and vertical, respectively, when we see the tubes in their "natural" direction (such as in the anode uniformity map).

Note that the tubes are not symmetric with respect to the exchange of x and y axes, or the rotation of (odd-integer multiples of) 90°. This is because of the construction of the dynodes, which has openings along the vertical (y) direction defined above.

2 Measurement setup

The experimental setup is shown in Figure 4. We use Hamamatsu diode laser PLP-02/041 as our light source. It consists of a precision pulser and a 405-nm diode laser head. The blue light is guided through a quartz fiber optic cable (core diameter 50 μm) to a Kuraray Y-11 wavelength-shifting fiber (0.83 mm in diameter), which is imbedded in a groove of a piece of plastic for mechanical stability. The light is converted in the fiber to a longer wavelength (green), and eventually reaches the face of the MA-PMT. There is an air gap of 1 - 2 mm between them. The other end of the WLS fiber goes to a conventional PMT (Hamamatsu H1161 with green-extended photocathode) for monitoring purposes. The MA-PMT is placed on a two-dimensional scanner so that effectively the fiber scans over the surface of the MA-PMT for uniformity measurements. The anode signals of the PMTs are measured with a CAMAC ADC (Kaizu 5010, nominal conversion factor of 0.3 pC per count) and read out through a PC. The ADC gate width is set to be 150 ns. The scanner movement is generated by pulse stepping motors and is controlled through the PC as well. The definition of our coordinate system is given in Figure 3.

3 Anode response uniformity

First, we want to measure the uniformity of PMT response among the 16 anode pixels. Hamamatsu provides us with their own measurement of anode uniformity. It is shown in Tables 3 and 4. They are a BACK VIEW [3], so top-left is Channel 1 and top-right is Channel 4. The uniformity given here is a relative one, normalized to the channel of the highest response (which is defined to be 100). One can see the numbers as low as 32, so there is a variation of up to a factor of three (max/min). The highest response tends to happen at the corners, and the lowest response at one of the four channels in the middle. We shall see that this is due to tube construction.

3.1 Anode uniformity at the center of the pixels

The current design of the CPR2 detector readout is to use one and only one WLS fiber per CPR channel, six of which correspond to one CEM tower (3 in ϕ, 2 in η). With this scheme the fibers will naturally go to the centers of the 16 pixels. Therefore we want to know the tube response at the 16 points on the surface of the tube.

In order to know where to shine the light on (to be more precise, where to move the tube under the Y-11 fiber), we need a reference point. We first scan the tube near the four channel in the middle, obtain data similar to those shown in Figures 12 and 13, and determine the center of the tube. Then we measure the response at the 16 points, corresponding to the centers of the pixels. The tube is usually said to have a pixel size of 4 mm by 4 mm with a spacing of 4.5 mm, but it is not strictly true. Moreover, the sizes, and even shapes, are different among the 16 pixels, as shown in Figure 5. The gap between the two neighboring anodes is always 0.3 mm.

Figure 6 shows an example (KA2460) of such measurements at the 16 points corresponding to the center of the channels. The amount of light is roughly 1000 photoelectrons. The applied high voltage is -550 V. There are three numbers shown in each of the small boxes in the figure. The first is the Hamamatsu number. The second is a Tsukuba number, the peak of the raw pulse height distributions (ADC counts) determined by a Gaussian fit. The third is also a Tsukuba number, which is obtained by dividing the second number by the peak pulse height of the reference tube. These two numbers differ very little, indicating the stability of the system during a measurement of 16 points. We also normalize the Tsukuba responses measured at 16 points to that of the "normalization" channel specified in Hamamatsu data sheet, which has a response of 100. In this case it is Channel 13. The resultant numbers are given in integers. If there exists more than one channel that has a response of 100 in Hamamatsu data sheet, we take the channel with the highest channel number. The channels at the corners (Channels 1, 4, 13 and 16) show a reasonably good agreement, but for the four channels in the middle (6, 7, 10 and 11), the Tsukuba numbers seem to be always higher than Hamamatsu, as much as 25%. We suspect that some systematic effects are involved here, and carry on measurements on more tubes.

Figure 7 shows a scatter plot of normalized anode responses, Tsukuba vs. Hamamatsu. There are nine tubes for which responses are measured, thus 144 entries in total, and there are nine "normalization point" entries at $(100, 100)$. All other points will serve as a judgement whether there are any correlations between the two sets of measurements. Correlations do exist, but the Tsukuba measurements tend to lie above the $y = x$ line for most of the channels. We split the scatter plot into four, depending on the channel number. It is shown in Figure 7(bottom). A linear fit is shown as the green line in each plot, which gives a slope that is larger than unity (when doing the fits the normalization channels are excluded). One can see that the correlations within the regions are much better and the points tend to lie close to the lines. The slope is largest for the channels in the middle, 6, 7, 10 and 11. For the regions "top/bottom" (Channels 2, 3, 14 and 15) and "left/right" (Channels 5, 9, 8 and 12), they are similar to each other and both smaller than the middle channels, but still are substantially different from unity. It is very close to unity for the "corner" channels, 1, 4, 13 and 16.

We first did not understand this behavior, but later we have learned that we are comparing apples and oranges here.

3.2 Anode uniformity : fine scan map

In order to understand the anode uniformity over the entire surface of the tube, we have taken data by scanning the points at 0.5 mm intervals. An example of such a measurement is shown in Figure 8 as a lego plot. This is a response of a single channel (Channel 1) as a function of the position (x, y) of the illumination point. The colored bands (25% intervals) are relative to the highest response point. The coordinate system is defined in Figure 3. The origin is arbitrary, and is away from the tube.

The response of all 16 channels from the same tube can be seen in Figure 9, where the contours of equal heights are drawn with 5% increments. The highest point within each channel is taken to be 100%. The 16 “squares” correspond to the anode pixels, and the crosses the centers. The large box is the tube glass envelope. To see the behavior more clearly, we show the contour plots again in Figures 10 and 11 so that the neighboring channels do not overlap. Also, we show their one-dimensional slices, the responses along one of the axes (e.g. x) while keeping the position on the other axis near the center of the pixels. They are shown in Figures 12 and 13. Solid vertical lines correspond to the pixel boundaries, and dashed lines the centers. Squares show the response of the reference tube. The data points in these one-dimensional plots are subsets of the two-dimensional fine-scan data.

One may notice that the regions of sensitivity extend beyond the pixel boundaries toward outside, notably on the top/bottom and left/right channels. The contour shapes are pretty close to circles for the four channels in the middle, but are skewed for other channels. The top/bottom channels seem to lack reflection symmetry about the vertical (y) axis that goes through the center in horizontal (x) direction. The same is true for the left/right channels regarding symmetry about the horizontal axis. The channels at the corners seem to possess symmetry about the diagonal axes, though.

They are not the characteristic inherent to this particular tube, rather common to all tubes. Plots from other tubes can be found at http://hep-www.px.tsukuba.ac.jp/~ukegawa/cpr2/. It seems likely that the behavior comes from tube construction. Perhaps the true sensitive area (cathodes and dynodes) is larger than the total anode area (18.1×18.1 mm^2) and the multiplied electrons may be able to exist outside the region. However, they eventually have to be absorbed somewhere. But there are no other electrodes surrounding outer channels, and so they may have no other choice but to end up on the anodes of the outer channels. It is just a conjecture, not confirmed with Hamamatsu.

Now, we take the responses in Figure 8 and add them all up, and redefine the sum as the channel response. This would be the response we would observe on this channel if we used a light source located far away from the tube and shone the entire surface of the cathode uniformly (“full illumination”). When we take this “integrated” channel responses of all channels from fine scan data and compare them with the Hamamatsu anode uniformity measurements, we have what is plotted in Figure 14. Data from all nine tubes are shown. Now the agreement is much better, and in all regions the points tend to lie much closer to the $y = x$ line. The reason for a better agreement is as follows. As shown earlier, the sensitive area of the outer channels extends over the anode pixel boundaries. Therefore, the integrated response at the outer channels will be larger than that for the channels in the middle, even if the responses at the centers of the pixels are the same. For the channels in the middle, the integrated responses will be smaller. So the Tsukuba numbers in Figure 7 tend to come down, most notably for the middle channels.

And it has turned out that it is indeed how Hamamatsu measures their anode uniformity [3]. So we *were* comparing apples and oranges in Figure 7. This also explains why the Hamamatsu normalization channel seems to be always located at the corners.

3.3 Back to anode uniformity at pixel centers

Now that we understand what the anode uniformity by Hamamatsu means and that it agrees better with our "integrarted' response measurement, we have more confidence in our anode response measured at the pixel centers shown previously. It is really what we are interested in, because the (new) design of the CPR2 detector employs only one fiber per readout channel, thus naturally the fiber goes to the center of the pixel.

The uniformity distribution from the nine tubes, 144 channels, is shown in Figure 15. To obtain the distribution, we have re-normalized the previously obtained responses at the centers of 16 channels (e.g. Figure 6) so that the average of the 16 responses within a given tube will be 1.0. This "re-normalization" process is necessary in order to get an unbiased estimate of the uniformity. We would have gotten an artificially wider distribution by simply using the numbers in Figure 7, if the normalization channel (the one with 100 in Hamamatsu anode uniformity map) had, for example, an anomalously high sensitivity. Physically the process corresponds to equalizing the average gains of all tubes, e.g. by adjusting HV settings on individual tubes.

The rms spread of the re-normalized distribution is about 10%. It is the channel-to-channel uniformity we would get for the real detector, namely the variation in raw response (e.g. MIP peak) from individual channels, if all other components of the detector (scintillators, fibers, connectors, electronics) were uniform.

For a comparison we show the distribution of anode responses calculated using the Hamamatsu measurements, with full illumination, in Figure 16. The rms spread here is 19%, which is substantially larger than that for the responses at the centers. For completeness, we also show the corresponding distribution from Tsukuba fine scan measurements.

4 Cross talk

The MA-PMT enables us to reduce the number of tubes while keeping a desired fine segmentation of the detector. However, we have to deal with the cross talk among the channels within the same tube. It is inevitable because of the tube construction. The Hamamatsu catalog lists a cross talk at a per cent level.

Our data with the light source at the center of the 16 channels serve for this purpose, because we always read out all 16 channels of the tube. The results are shown in Figure 17. The leakage to the most adjacent neighbors (those sharing the sides) is at 2 to 3 per cent level, while the diagonal leakage is around 0.5%.

We stress that the cross talk depends on the detector construction, namely how we guide the fibers to the photocathode. The light exiting the fiber has a finite cone angle that is determined by the index of refraction, and the spread at the depth of photocathode is what creates the cross talk. Therefore, the distance from the edge of the fiber to the tube glass envelope matters, as well as the thickness of the glass, which we have no control over. In our measurement setup, we have to have a finite space between the fiber and the glass envelope, because we have to move the tube relative to the fiber. That distance is of order 1 mm. In the real detector this distance will be almost zero, so the cross talk numbers given above will be an upper limit.

5 Pulse linearity

There are two kinds of linearity we have to consider. The first is the non-linearity that is caused by the "saturation" of the bleeder currents. The measure for this non-linearity will be the total anode current, which depends on luminosity and occupancy as well as the size of single pulses. The other is pulse non-linearity, which has nothing to do with the bleeder circuit saturation. This is caused by space-charge effect at the final few stages of the dynodes and the anode. The effect is known to be solved, at least partially, with the so-called "tapered" bases, by applying higher voltages at these stages and forcing the electrons to move quickly to the next stage of the dynodes or to the anode so that the electrons do not stay at a place in space for a long time. The tube with this tapered base circuit has the name H6568-10, "10" because it has a factor of ten better dynamic range. Our tubes are of normal bases.

Hamamatsu catalog shows the pulse linearity for H6568 and H6568-10 models as a function of the anode current. For H6568, the response deviates from a linear behavior by 2% at an anode current of 0.5 mA. For H6568-10, it is 5 mA. We might want to talk things in terms of the output charge, and for that purpose we need to know the pulse width. The shape of the signal at CPR will be determined by the decay time of the Y-11 wavelength shifter, which is longer than scintillation light, but is still fast, of order 10 ns. If we operate the tube at a gain of 10^6, a 10 photoelectron MIP will produce a charge of 1.6 pC. If this amount of charge is collected by the tube with a time duration of 10 ns, the average current will be $I_{\text{pulse}} = 1.6$ pC $/10$ ns $= 0.16$ mA. So the 2% saturation point is only at 3 MIPs. Maybe the 10 ns pulse width assumed here is shorter than reality, but it is clear that we are not far from the saturation point with the linear base.

Therefore, we have measured the pulse linearity with our setup. We *do* use light from a Y-11 WLS fiber, so we should be close to what we will have in the real CPR detector. To measure the pulse linearity, we change the high voltage applied to the tube and see how the collected charge changes. It is known that the gain changes with a certain power of the HV value, so if we plot charge vs. HV on log-log scales, it would lie on a line, and a deviation from it would indicate saturations. Figure 18 shows results of such a measurement. There are data points from three tubes, KA2580, KA2626 and KA2418. The first two are from the ten CPR2 R&D tubes. And KA2418 is one of the tubes purchased by our colleagues at KEK and used for a prototype JCL calorimeter test beam in fall 2002, and it is of the H6568-10 model (tapered base). Two sets of points exist for each tube and correspond to different amounts of light, with an intention of producing roughly 10 and 1000 photoelectrons, using neutral density (ND) filter of $0.5 + 0.5 = 1.0$ and $1.0 + 2.0 = 3.0$. A filter with index x should reduce the amount of light by a factor of 10^x.

First, one can easily notice that the H6568-10 tube has a much better linearity response than H6568, although the gains are lower. The H6568 tubes seem already saturated at -800 V, at which point the tube gain (from Hamamatsu data sheet) is 5.1×10^6 and 7.0×10^6.

Another thing one may notice is that the saturation seem to occur at different output charges for the two amounts of light. The saturation for a larger amount of light does not appear until later, or at a larger pulse. This behavior might sound peculiar, because one would expect that the current should be the same for a given output charge, and if the saturation is governed by the anode current, it should happen at the same scale on the vertical axis, output charge, for the two conditions.

When we performed single photoelectron measurements, we have found out that we should really be concerned with the *peak* anode current, instead of the current averaged over the duration of the pulse, and that the peak current indeed depends on the amount of light (even if the output charges are the same).

The point will become clear if you consider an extreme case of measuring single photoelectrons. When one and only one photoelectron is produced at the photocathode and followed by multiplications in the dynode stages, the resultant pulse shape will be very narrow, of order 1 ns, because the transit time spread (TTS) of the tube is only at 300 ps. Of course the absolute timing with respect to the passage of a particle is governed by the decay time of the Y-11 wavelength shifter, so there will be an event-by-event variation of order 10 ns. However, for a given single photoelectron pulse, the pulse width is of order 1 ns, not 10 ns. On the other hand, when we measure the pulse of a large number of photoelectrons N, it is a sum of N pulses, each of which has the pulse shape of single photoelectrons but starts at different timing, spread over the decay time of Y-11.

The peak anode currents will then be different in the two cases, even if they had the same total charge.

Therefore, we first need to produce a condition similar to the real detector. We expect one MIP will produce roughly 10 photoelectrons. The curve with the ND filter of 3.0 $(1.0 + 2.0)$ is close to this condition, and it is already saturated at -800 V, as mentioned earlier.

Figures 19 through 21 show scope photos of the pulse shapes observed with one of the channels of KA2626, at a high voltage of -700 V. The amount of light corresponds roughly to 1000, 10 and single photoelectrons, respectively. There are two pictures in each figure (except for the single photoelectron case); one is obtained by triggering the scope by the MA-PMT pulse itself (self-trigger), and the other is triggered by the laser trigger pulse. Both show average pulse shapes, accumulating 1000 sweeps.

One can clearly observe that the widths of self-triggered pulses are different for different amount of light. The FWHM is only 2.5 ns for single photoelectrons, less than 7 ns for 10 photoelectrons, and 15 ns for 1000 photoelectrons. If we use this 7 ns as the pulse width, the anode current of a 1.6 pC pulse will be 0.23 mA, already close to the Hamamatsu 2% saturation point. And it seems consistent with the linearity plot, Figure 18. When we trigger the scope with the timing of laser light emission, the width for the 10-photoelectron pulses is wider, over 10 ns. For the 1000-photoelectron case, the shape is virtually independent of the way how you trigger the pulses, both around 15 ns. It indicates that 1000 is a large enough number so the pulse width is governed predominantly by the Y-11 decay time. The 10-photoelectron case is somewhere in between, and indeed there are quite large fluctuations from one event to another, as can be seen in single-shot pictures shown in Figure 22.

It is certainly desirable to keep linearity at larger pulse heights, let alone one MIP, so we conclude that the tapered base is the way to go.

6 Single photoelectron peaks and the absolute gain

The absolute gains of PMTs can be determined if one can observe the pulses of single photoelectrons, which requires high gains so that the peak can be separated from pedestals. We thus apply high voltage as high as -1000 V.

Figure 23 shows an example of ADC distributions taken with additional ND filters (total of 4.5). A LeCroy ADC (2249A, 0.25 pC per count) is used. The single photoelectron peak is clearly visible.

We have to be careful when we estimate absolute gains from these distributions, because the non-linearity is a concern here as well. The high voltage dependence of single photoelectron peaks is already shown in Figure 18. It cannot cover possible non-saturated region at lower voltages, so we cannot see the whole picture, but local slopes of the curve where data point exist indicate the single photoelectron pulses are saturated too. It can also explain why the pulse height distribution is skewed, narrower on the high side, at the high end, 1000 V, while it looks more symmetric at 800 V. We are hoping to be able to make some estimates, and will update this note when they become available.

Meanwhile, tapered-base tubes have a better linearity behavior, so we show their data. However, their lower gains limit us to see single photoelectron peaks only around 1000 V. Figure 24 shows a comparison of absolute gains determined with single photoelectron peaks (Tsukuba) and with cathode and anode currents (Hamamatsu). The single photoelectron measurements are done at 1000 V and gains are extrapolated to 800 V. The agreement is not perfect, but they are the same at 20% level on the average.

7 Conclusions

The conclusions are summarized as follows.

- Anode uniformity
  If we use the tube the way we would for CPR2, the relevant quantity is the uniformity at the centers of the pixels, which is different from and is much better than the one provided in Hamamatsu data sheets. The rms spread is about 10%.

- Cross talk
  It should be less than about 3% on direct neighbors.

- Pulse linearity
  We need a tapered base. In particular care has to be taken when we will observe pulses with small number of photoelectrons.

- Single photoelectron peaks and absolute gain
  Hope ours agree with Hamamatsu. Again, saturation effects have to be taken care of.

H6568 should be adequate for CPR2, but the tapered base version, H6568-10, is highly desirable or even necessary. Other changes considered for the production tubes are listed in Appendix A.

Appendices

A Changes considered for the production tubes

CPR2 will have a total channel count of $64 \times 48 = 3072$, or 192 MA-PMT tubes. The procurement plan spans over three Japanese fiscal years, 2002, 2003 and 2004. And for the year 2002 (ending March 31, 2003) 40 tubes are planned, including ten "pre-production" tubes. Technical issues and the changes considered accordingly can be summarized as follows.

- Pulse linearity and the choice of base circuit.
  This is more of a concern for electrons than for photons. We have to operate the tubes at high enough gains so that the MIP peak is well separated from the pedestal. Ten photoelectrons and a gain of 10^6 will give a charge of 1.6 pC for a MIP. Since SMQIE electronics has a resolution of 20 fC per count and a pedestal width of less than one count, 80 counts per MIP should be good enough. Now the issue is whether early-showered electrons will show saturations or not. From the TDR, one can see that the $W^{\pm}$ electrons can give pulse heights up to 50 MIPs. This corresponds to 80 pC if the gain is 10^6.

- Anode resistors.
  The anode resistors are R18 - R33 in Figure 2. They have been known to cause trouble to the QIE (and SMQIE) electronics used at CDF. The plan is to remove these resistors in the production tubes. Note their absence in Figure 26.

  However, a care has to be taken, because the anode signal lines are floated and there is nothing that determines their DC level within the base circuit itself. When we apply a high voltage to a tube without connecting the anodes to anything, the charges will pile up on the anodes. If you then make a connection, e.g. to an electronics, the accumulated charge could damage the electronics. The second point concerns the ground level. The anode ground will be determined by the readout electronics.

- Ground-loop breaker.
  It is R19 in the drawing (Figure 26), 300 Ω.

- Signal and dynode connections.
  Pins will be placed at the end of the tubes, instead of coaxial cables coming out. The signals are carried by flat cables over a short distance within the PMT box, and then transmitted through coaxial cables.

  The HV connection remains an RG-147 cable.

B Pre-production tubes

The changes discussed in Appendix A have been communicated to Hamamatsu, and they have prepared a new version of the tube, H8711A-10MOD. The mechanical and electrical drawings are reproduced in Figures 25 and 26.

The transition from the pins on the tube to a flat cable connector, such as Samtec IDSD-08, is not completely solved in the pre-production tubes. The pins by Hamamatsu are probably too short for IDSD connectors. Hamamatsu is now trying pins that should mate with IDSD, such as TSW-108-07-?-D.

Ten tubes were ordered in October 2002, and as we are writing this note they are delivered (on December 24, 2002).

References

[1] CDF Collaboration, Run-IIb Technical Design Report.

[2] S. Lami, S. Kuhlmann, K. Hatakeyama and M. Gallinaro, CDF 6094.

[3] T. Okada, Electron Tube Department, Hamamatsu Photonics KK, private communications.

試験成績表

PAGE 001 OF 001

2002 年 2 月 8 日

納入先 筑波大学 殿

品名 光電子増倍管： H6568

御注文番号

納入本数 完納 10 本

受注方法 1 (1.受注品 2.代替品 3.サンプル品 4.貸出品)

浜松ホトニクス株式会社
電子管事業本部
〒438-0193 静岡県磐田郡豊岡村下神増314-5
☎ (0539) 62−5245
ファックス (0539) 62−2205

NOTES

1,2,4 光源は、2856 K 標準タングステンランプ。
2.3 印加電圧： 800 V
電極電圧配分比： 別紙参照
測定は、全てのAnodeを束ねた状態で行われた。
4 使用フィルタ： コーニング CS 5-58 (1/2厚)

参照規格： EIAJ･ET61A 光電管及び光電子増倍管試験方法

Serial Number	(1) 陰極感度 (Sk) μA/lm	(2) 陽極感度 (Sp) A/lm	(3) 陽極暗電流 (Idb) nA	(4) 陰極青感度指数 (Skb)
KA2571	94.0	729.0	2.65	9.88
KA2633	85.6	530.0	3.06	8.72
KA2467	103.0	580.0	3.68	9.97
KA2419	96.8	530.0	0.23	8.79
KA2402	96.3	629.0	2.31	9.53
KA2527	85.6	646.0	0.73	9.93
KA2523	94.2	729.0	2.98	9.53
KA2580	91.9	464.0	1.34	9.92
KA2626	91.9	646.0	5.40	9.50
KA2461	103.0	596.0	2.71	9.90

検査印

HAMAMATSU

Table 1: Hamamatsu data sheet for ten H6568 tubes. Sk is cathode sensitivity, Sp is anode sensitivity. All measured at −800 V, and with all anode channels ganged into one readout.

試験成績表

PAGE 001 OF 001

2002 年 2 月 8 日

納入先 筑波大学 殿

浜松ホトニクス株式会社
電子管事業本部
〒438-0193 静岡県磐田郡豊岡村下神増314-5
☎ (0539) 62 5245
ファックス (0539) 62−2205

品名 光電子増倍管： H6568MOD

御注文番号

納入本数 完納 10 本

受注方法 1
1.受注品
2.代替品
3.サンプル品
4.貸与品

NOTES

1,2,4 光源は、2856 K 標準タングステンランプ。
2,3 印加電圧： 800 V
電極電圧配分比： 別紙参照
測定は、全てのAnodeを束ねた状態で行われた。
4 使用フィルタ： コーニング CS 5-58 (1/2厚)

参照規格： EIAJ・ET61A 光電管及び光電子増倍管試験方法

Serial Number	(1) 陰極感度 (Sk) μA/lm	(2) 陽極感度 (Sp) A/lm	(3) 陽極暗電流 (Idb) nA	(4) 陰極青感度指数 (Skb)
KA2440	98.4	530.0	9.24	9.94
KA2409	109.0	531.0	1.59	9.92
KA2437	105.0	596.0	10.21	9.92
KA2399	87.6	447.0	0.70	9.10
KA2443	92.0	431.0	0.21	9.91
KA1695	111.0	514.0	4.55	10.60
KA2460	87.7	431.0	0.18	9.52
KA2431	98.4	364.0	2.84	9.12
KA1491	105.0	308.0	0.15	9.93
KA2319	98.2	310.0	0.80	9.86

検査印

HAMAMATSU

Table 2: Hamamatsu data sheet for ten H6568MOD tubes.

H6568 Anode Uniformity

Light Source : W-LAMP+5-58(400nm)
Bleeder Ratio : 1:1:1:1...1:1:1
Ebb : 800(V)

Serial No.: KA2571

83	70	74	91
73	55	55	73
78	58	58	74
95	73	73	100

Serial No.: KA2633

94	84	80	100
98	91	80	83
99	88	82	83
100	89	85	94

Serial No.: KA2467

84	83	86	95
82	72	66	78
81	78	72	83
98	93	97	100

Serial No.: KA2419

86	83	89	99
79	66	65	86
76	66	63	86
85	83	86	100

Serial No.: KA2402

91	91	86	95
76	63	53	61
80	60	51	70
100	89	89	100

Serial No.: KA2527

91	87	79	91
79	77	74	78
80	75	75	77
100	85	79	92

Serial No.: KA2523

92	86	85	100
87	70	64	81
90	74	67	82
92	88	83	98

Serial No.: KA2580

84	78	76	85
76	69	70	76
75	72	75	78
98	90	89	100

Serial No.: KA2626

87	76	74	90
77	70	71	76
80	75	73	81
98	82	81	100

Serial No.: KA2461

91	87	88	100
73	65	66	75
75	68	68	75
100	84	82	96

HAMAMATSU
HAMAMATSU PHOTONICS K.K., Electron Tube Center

Table 3: Hamamatsu measurement of anode uniformity for ten H6568 tubes. This is a BACK VIEW, so top-left is channel 1 and top-right is channel 4.

H6568MOD Anode Uniformity

Light Source : W-LAMP+5-58(400nm)
Bleeder Ratio : 1:1:1:1...1:1:1
Ebb : 800(V)

Serial No.: KA2440

90	77	72	85
74	60	63	71
77	63	67	76
100	92	84	95

Serial No.: KA2409

81	78	73	84
76	81	67	81
70	77	76	88
75	72	77	100

Serial No.: KA2437

100	90	85	91
87	77	66	77
82	73	67	85
94	86	84	99

Serial No.: KA2399

93	82	82	100
76	53	59	83
79	54	60	81
89	72	75	88

Serial No.: KA2443

82	79	85	100
66	67	65	74
65	62	64	74
83	75	74	90

Serial No.: KA1695

74	65	59	68
64	32	33	57
70	39	37	64
96	89	84	100

Serial No.: KA2460

87	79	75	90
78	64	60	76
78	64	59	66
100	83	80	95

Serial No.: KA2431

81	72	73	85
71	61	64	73
67	65	70	79
83	70	75	100

Serial No.: KA1491

74	61	60	100
51	34	34	63
48	32	33	65
58	51	56	91

Serial No.: KA2319

91	70	74	100
66	38	38	71
62	32	35	65
90	57	60	91

HAMAMATSU
HAMAMATSU PHOTONICS K.K. Electron Tube Center

Table 4: Same as the previous Table but for ten H6568MOD tubes.

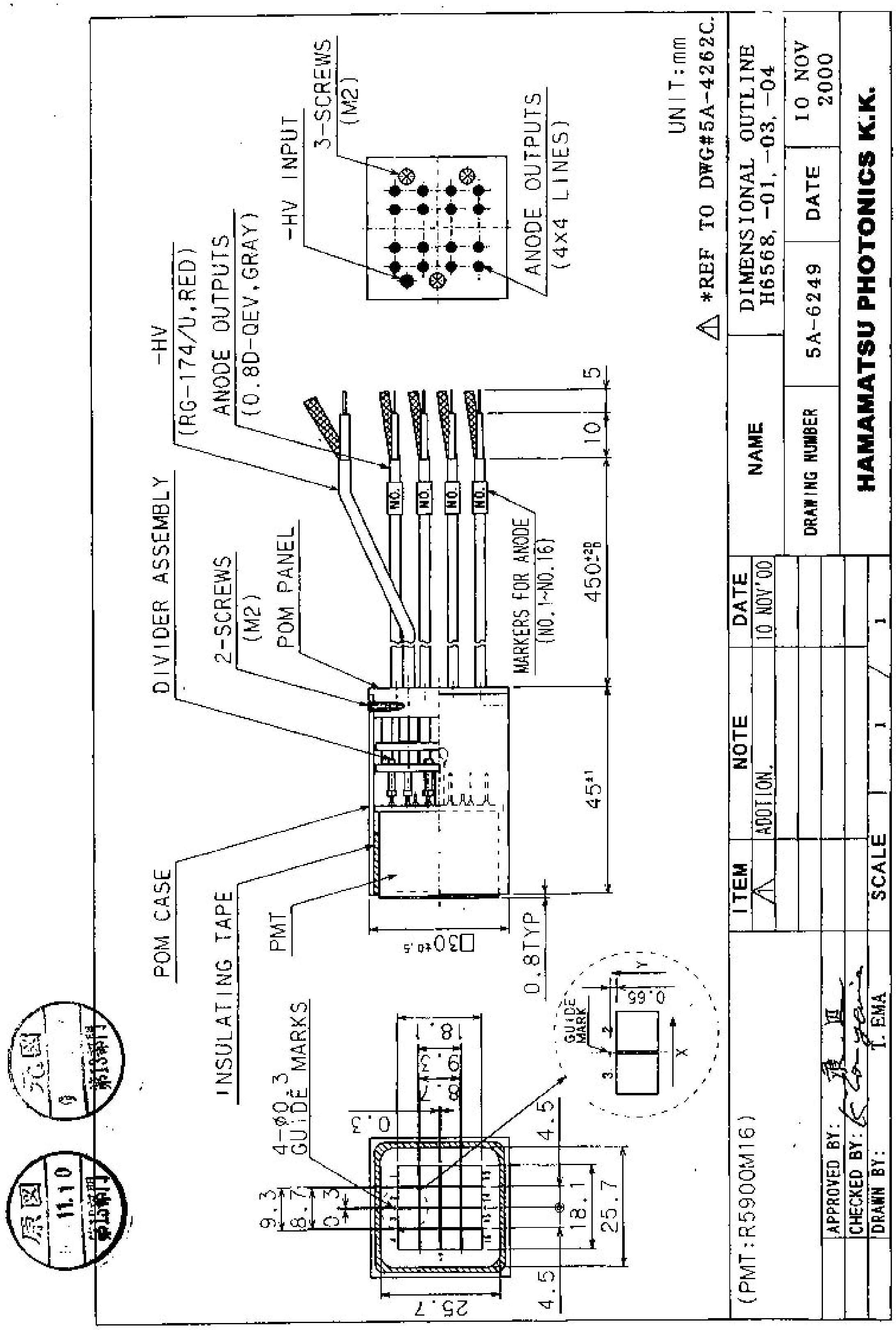

Figure 1: Mechanical drawing of the model H6568 (by Hamamatsu).

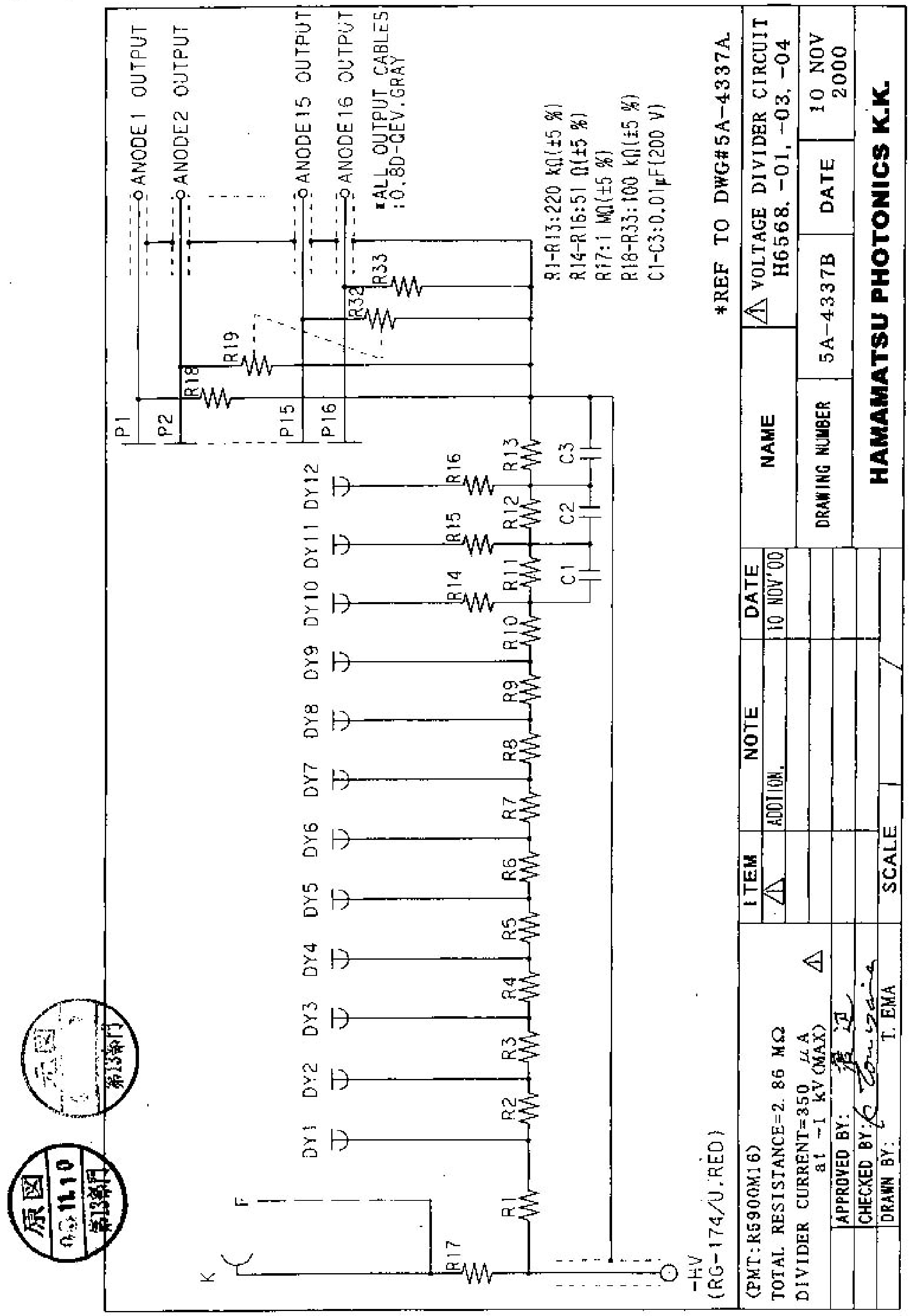

Figure 2: Electrical drawing of the model H6568 (by Hamamatsu).

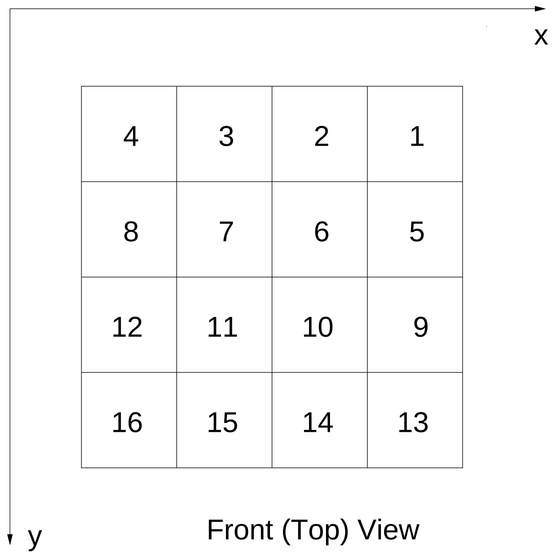

Figure 3: Definition of the channel numbers when looking into the photocathode (front view). Also the definition of the coordinate system is given.

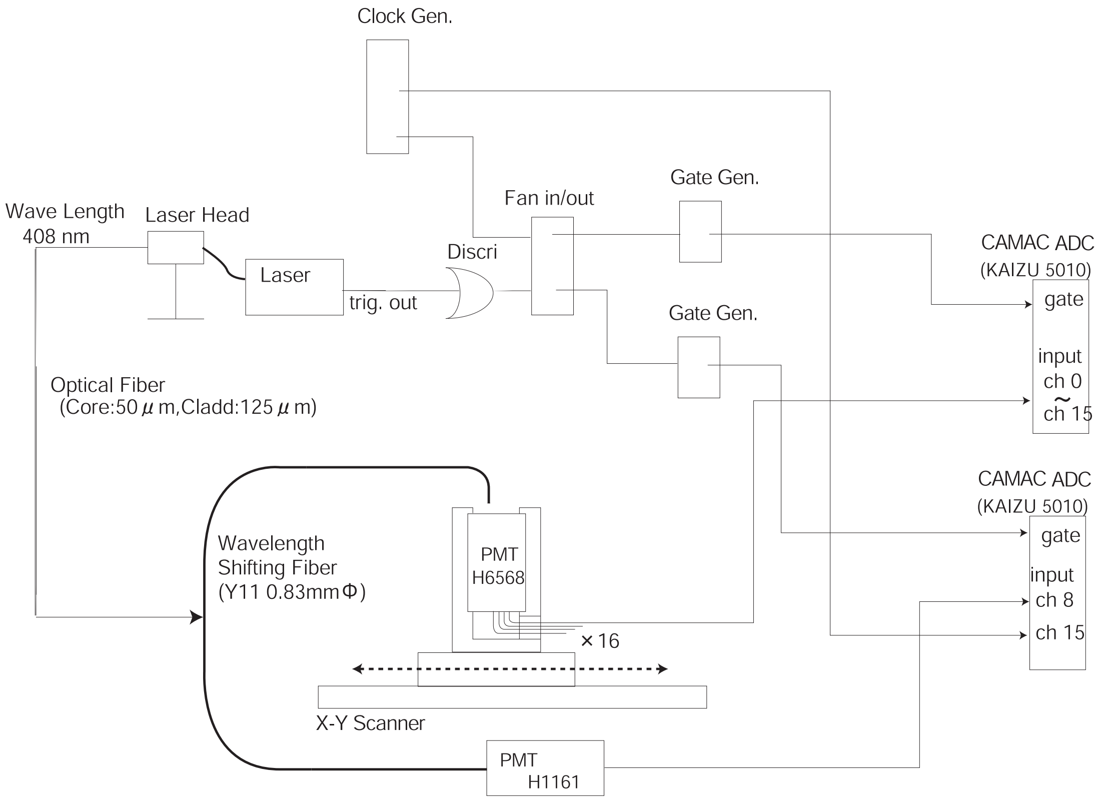

Figure 4: Experimental setup for measurements of multi-anode PMTs.

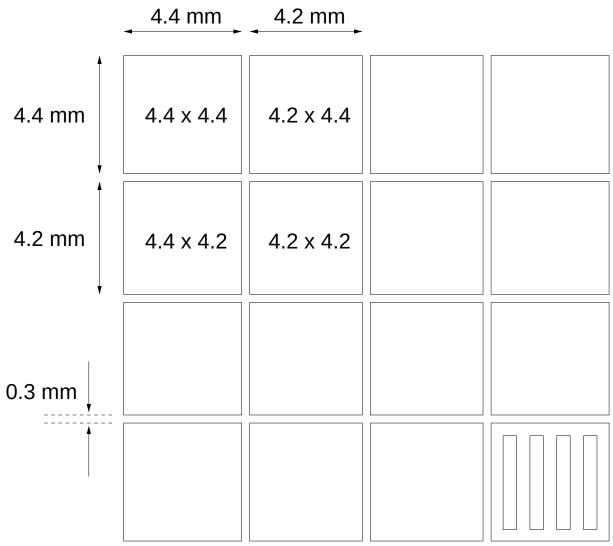

Figure 5: Sizes and shapes of anode pixels, in units of mm.

ka2460:120502

ch1 hamamatsu=87 ADC=36.56±0.08 97 mapmt/h1161 =0.698±0.001 97	ch2 79 34.07±0.06 90 0.653±0.001 90	ch3 75 32.54±0.06 86 0.623±0.001 86	ch4 90 35.16±0.07 93 0.672±0.001 93
ch5 78 36.53±0.06 97 0.699±0.001 97	ch6 64 35.22±0.07 93 0.674±0.001 93	ch7 60 30.94±0.07 82 0.592±0.001 82	ch8 76 31.15±0.07 82 0.597±0.001 82
ch9 78 36.17±0.06 96 0.694±0.001 96	ch10 64 35.21±0.06 93 0.674±0.001 93	ch11 59 29.06±0.07 77 0.557±0.001 77	ch12 66 27.18±0.07 72 0.521±0.001 72
ch13 100 37.65±0.08 100 0.72±0.001 100	ch14 83 35.64±0.06 94 0.682±0.001 94	ch15 80 33.76±0.06 89 0.647±0.001 89	ch16 95 34.67±0.06 92 0.663±0.001 92

Figure 6: Responses at the center of 16 channels. Normalized to that of the channel with maximum response as specified by Hamamatsu anode uniformity data. Two sets of numbers are the raw ADC counts and the ones divided by that of the reference tube. They differ very little.

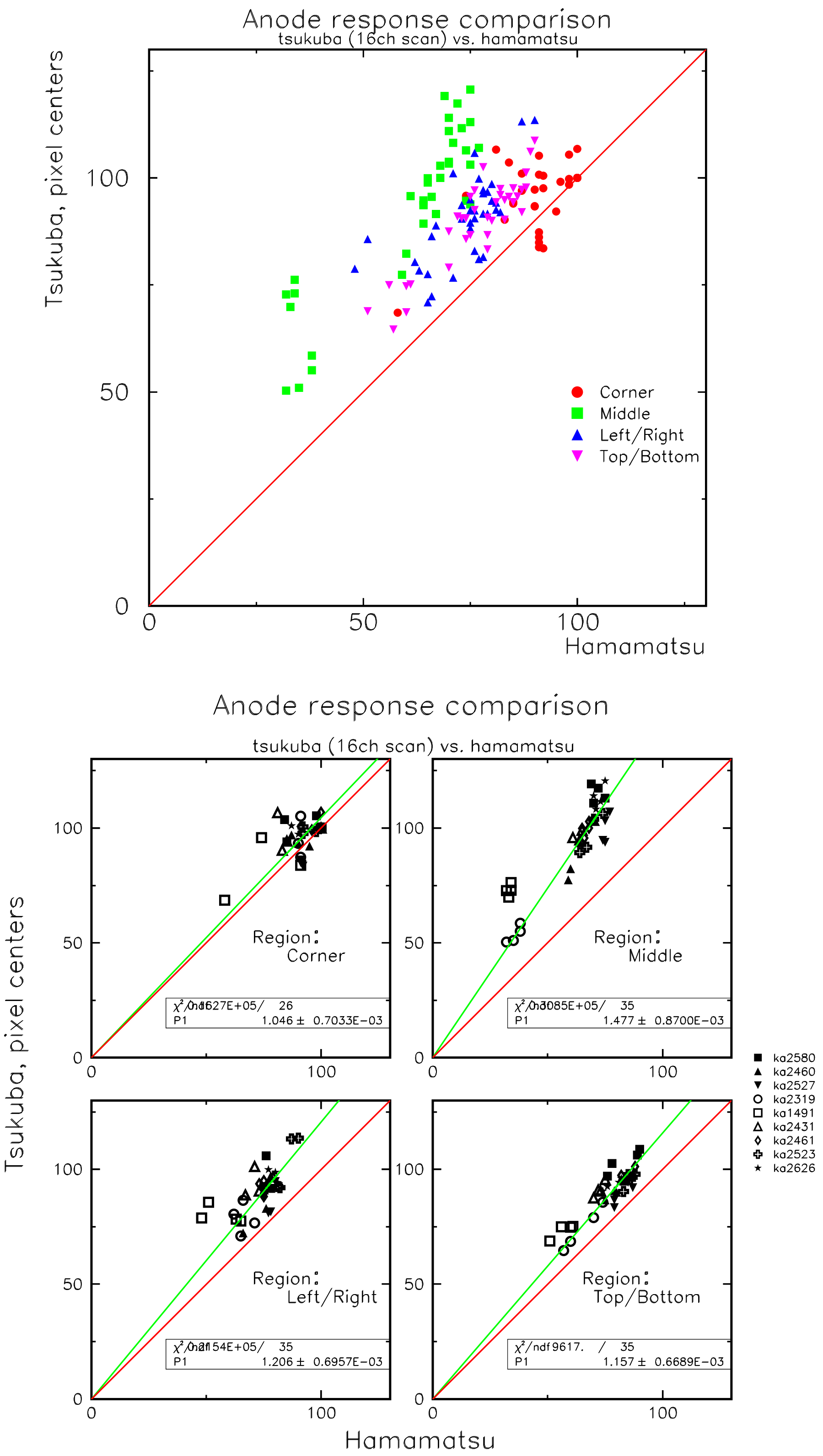

Figure 7: Comparison of Tsukuba measurements of responses at the centers of 16 channels to Hamamatsu anode uniformity data for nine tubes. Normalized to the channel with maximum response as specified in Hamamatsu anode uniformity data, so there are nine entries at $(100, 100)$. Top: all channels. Bottom: divided into four regions.

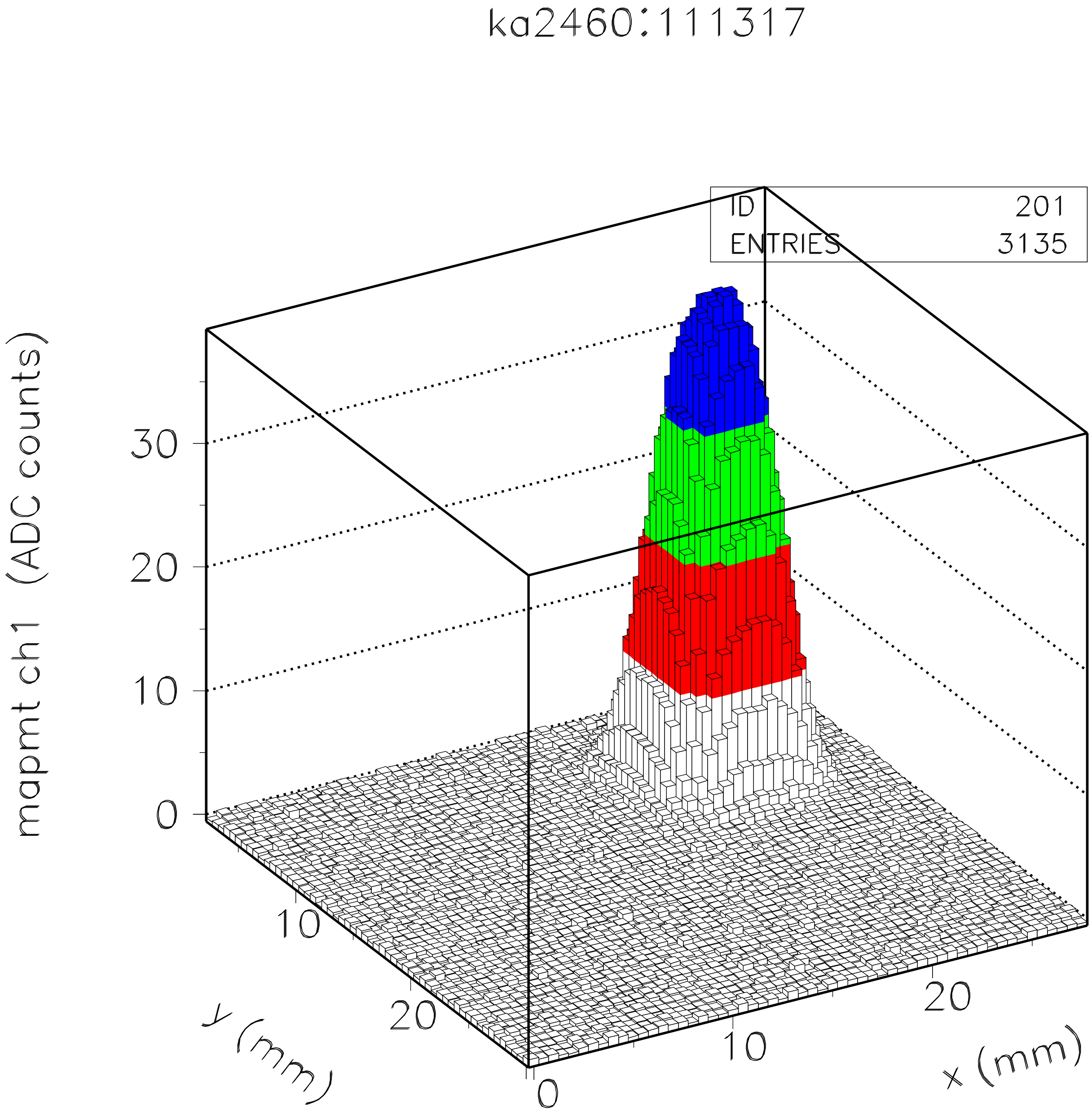

Figure 8: Response of a single channel (Channel 1, KA2460)) as a function of the illumination position (x, y).

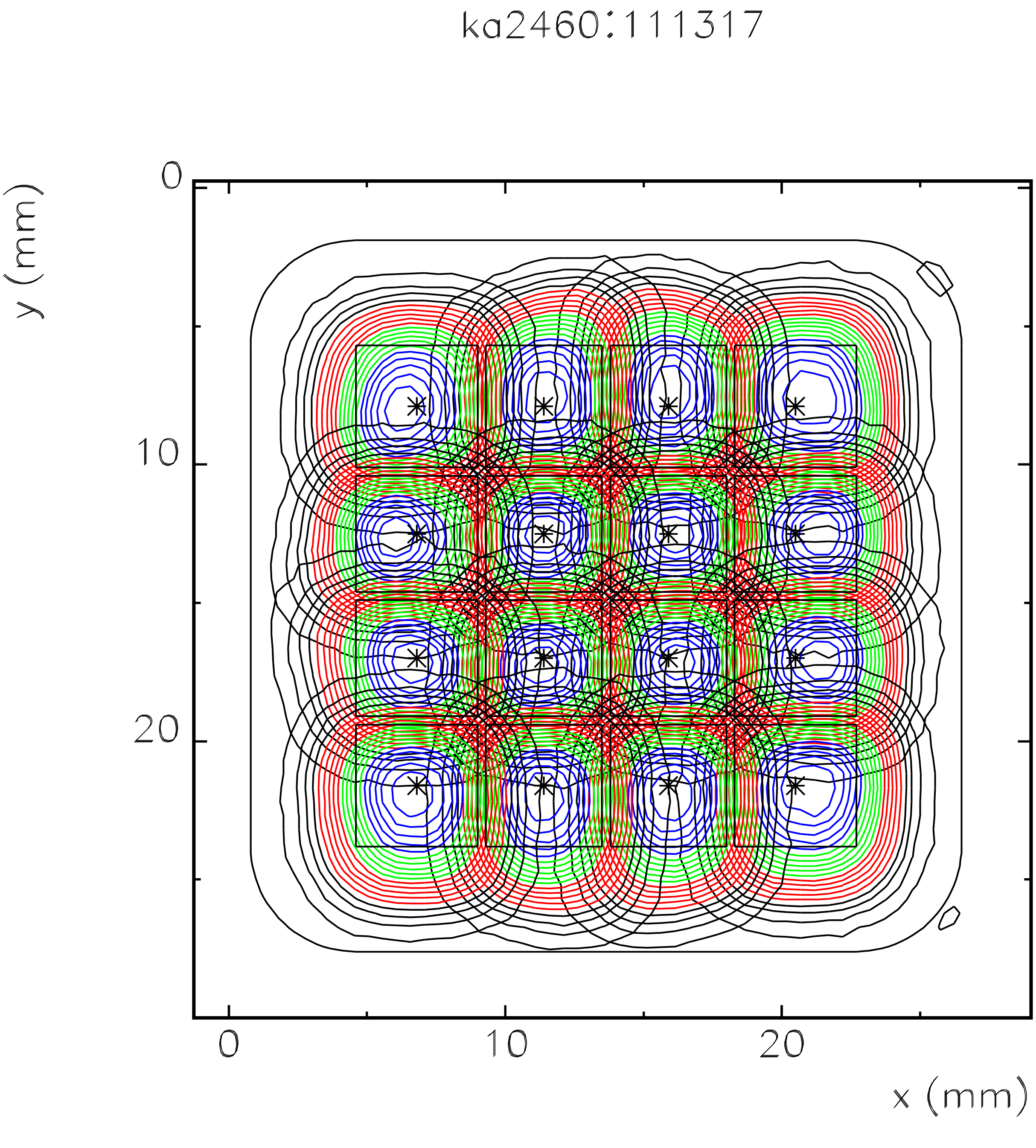

Figure 9: Response of 16 channels as a function of the illumination position (x, y). Pulse heights are shown as contours of 5% increments, relative to the highest point within individual channels.

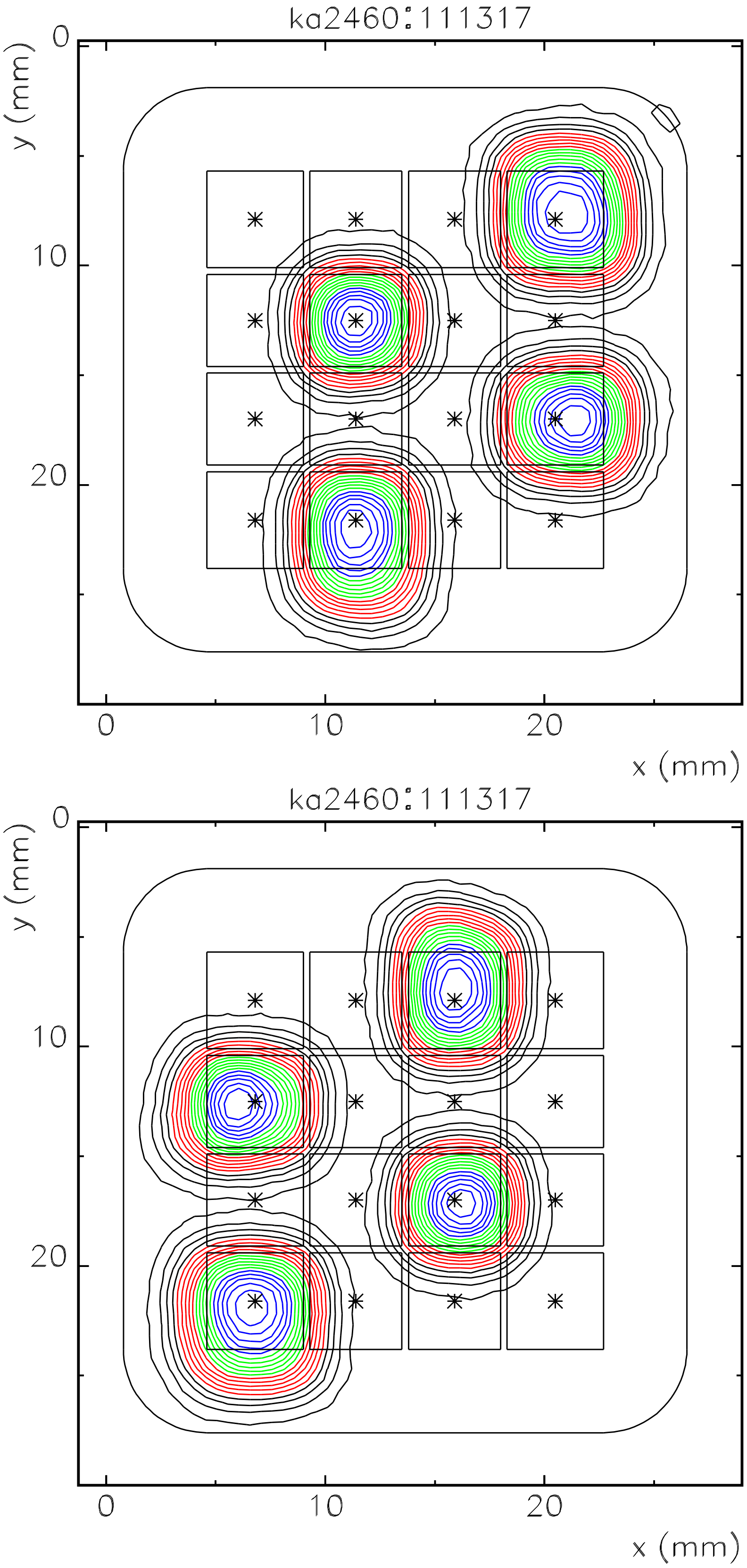

Figure 10: Same as the previous Figure but only four channels are selected in each plot.

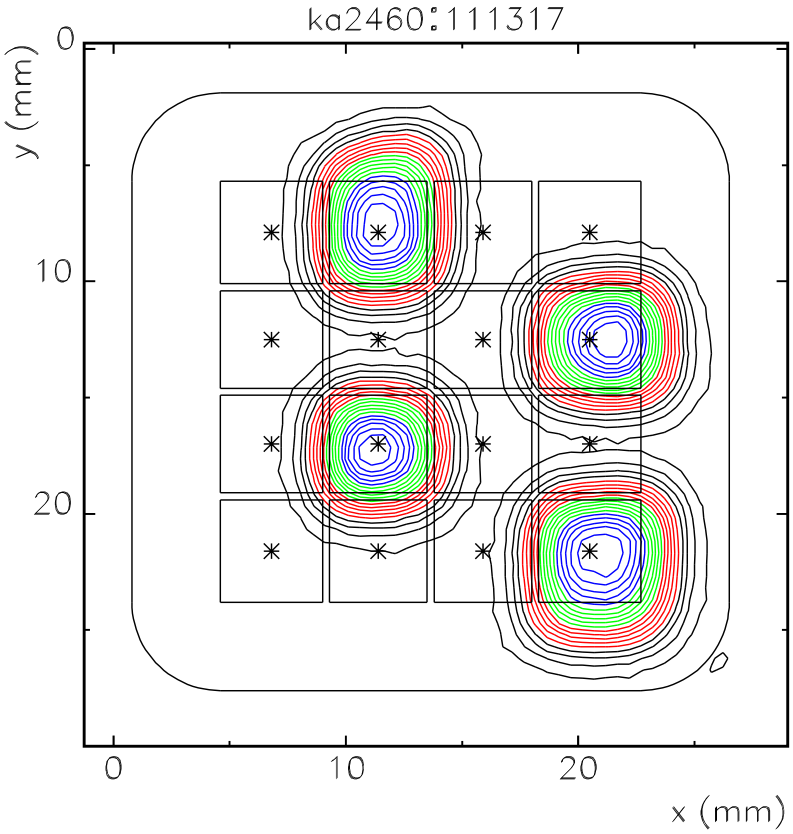

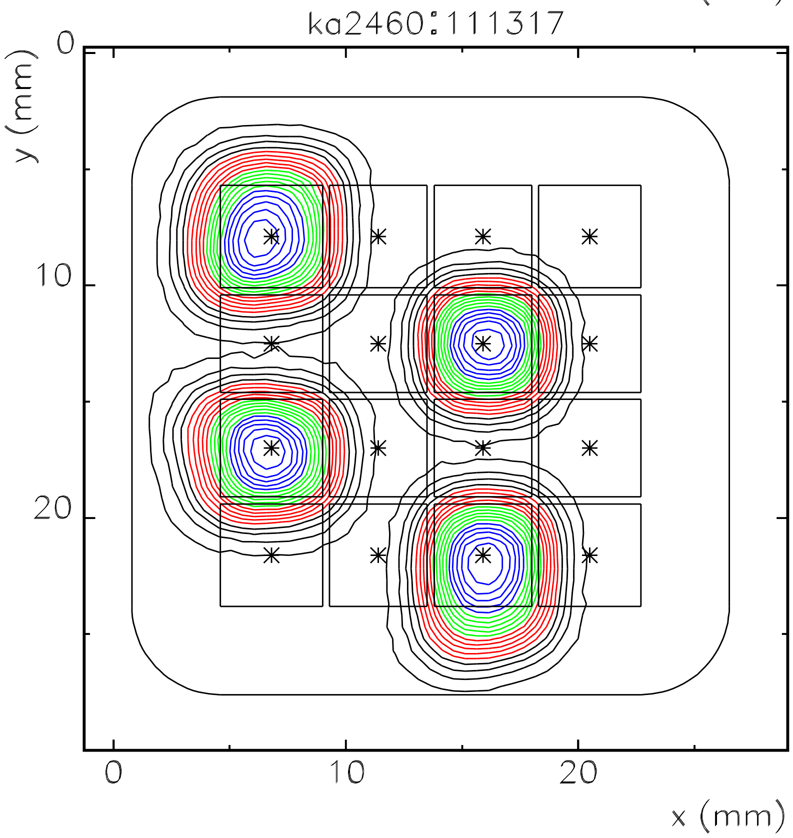

Figure 11: Same as the previous Figure, other four-channel sets are shown.

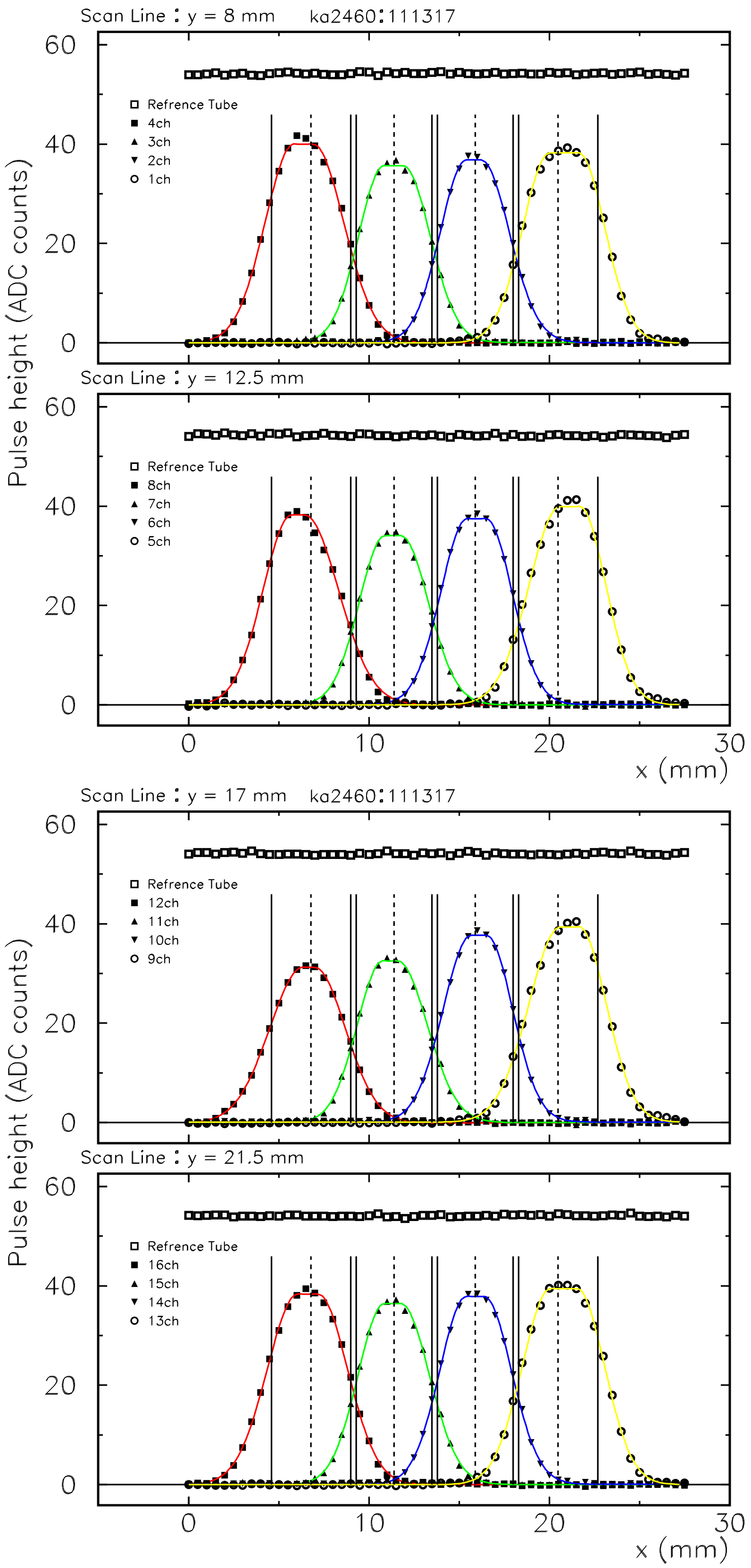

Figure 12: Response of 4 channels in a given row as a function of the illumination position x while keeping the position y near the center of the pixels.

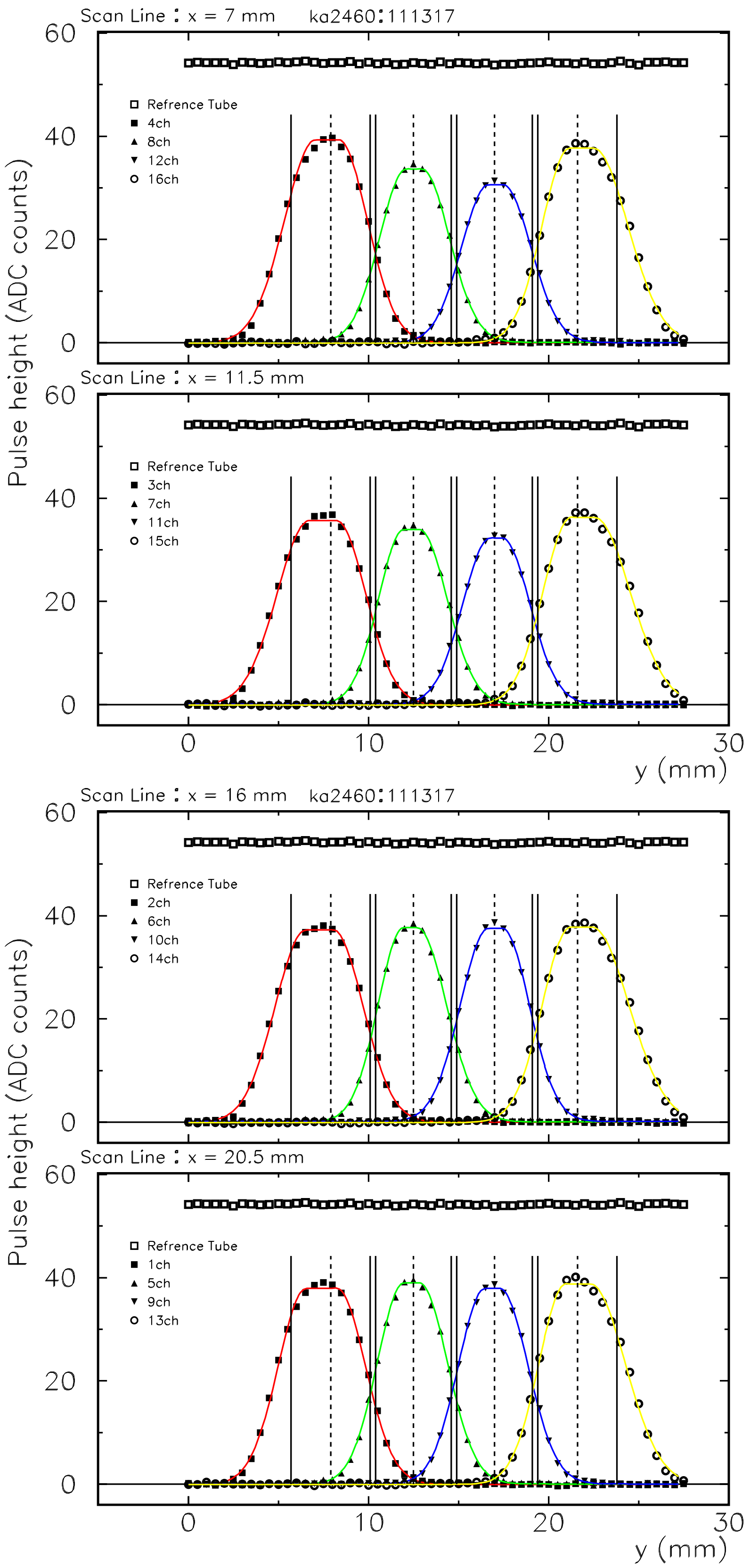

Figure 13: Response of 4 channels in a given column as a function of the illumination position y while keeping the position x near the center of the pixels.

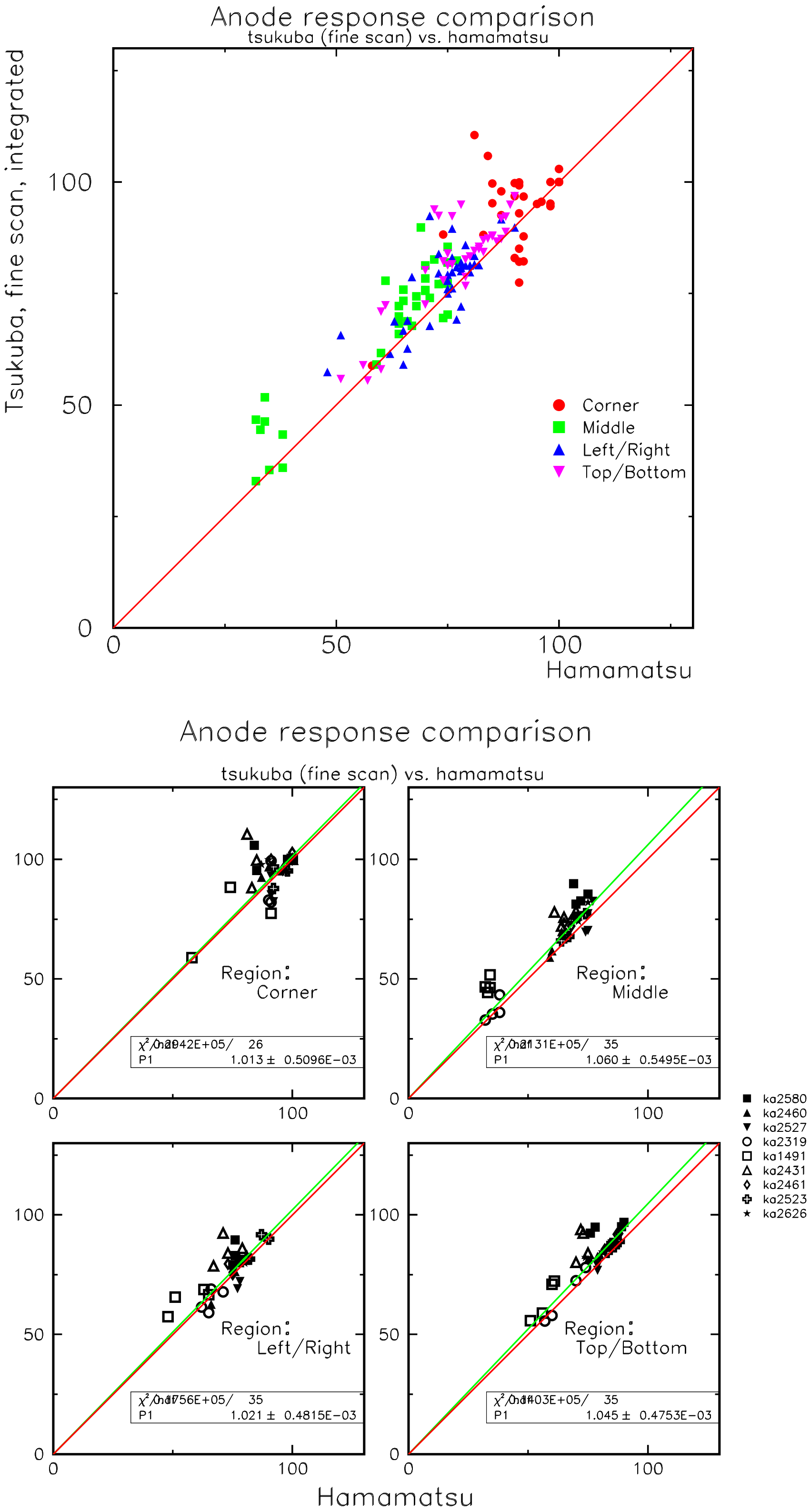

Figure 14: Comparison of the "integrated" anode responses from Tsukuba fine-scan data to Hamamatsu anode uniformity data. Top: all channels. Bottom: divided into four regions.

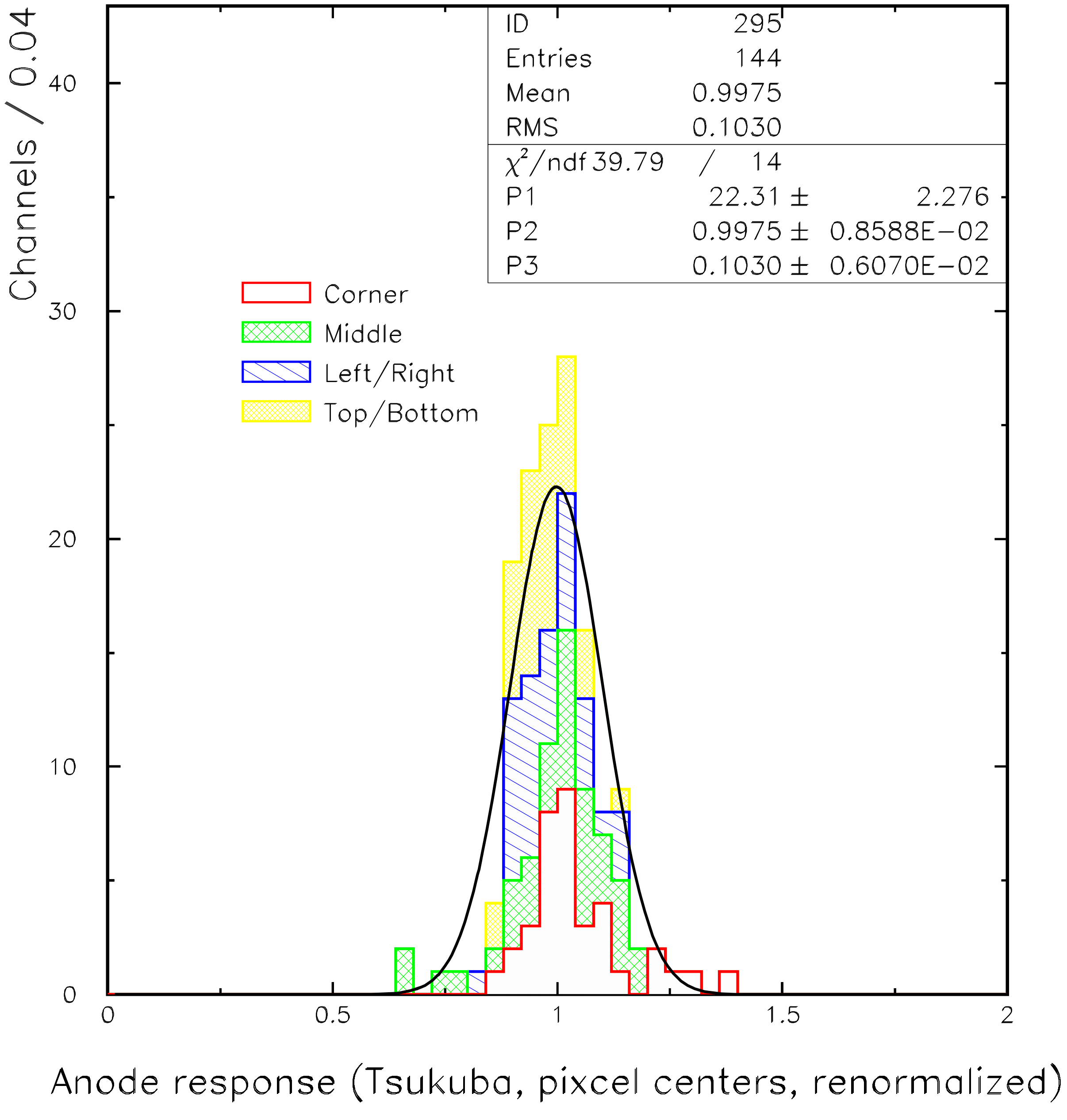

Figure 15: Distribution of re-normalized anode responses at the center of the pixels, as measured at Tsukuba for nine tubes (spot illumination).

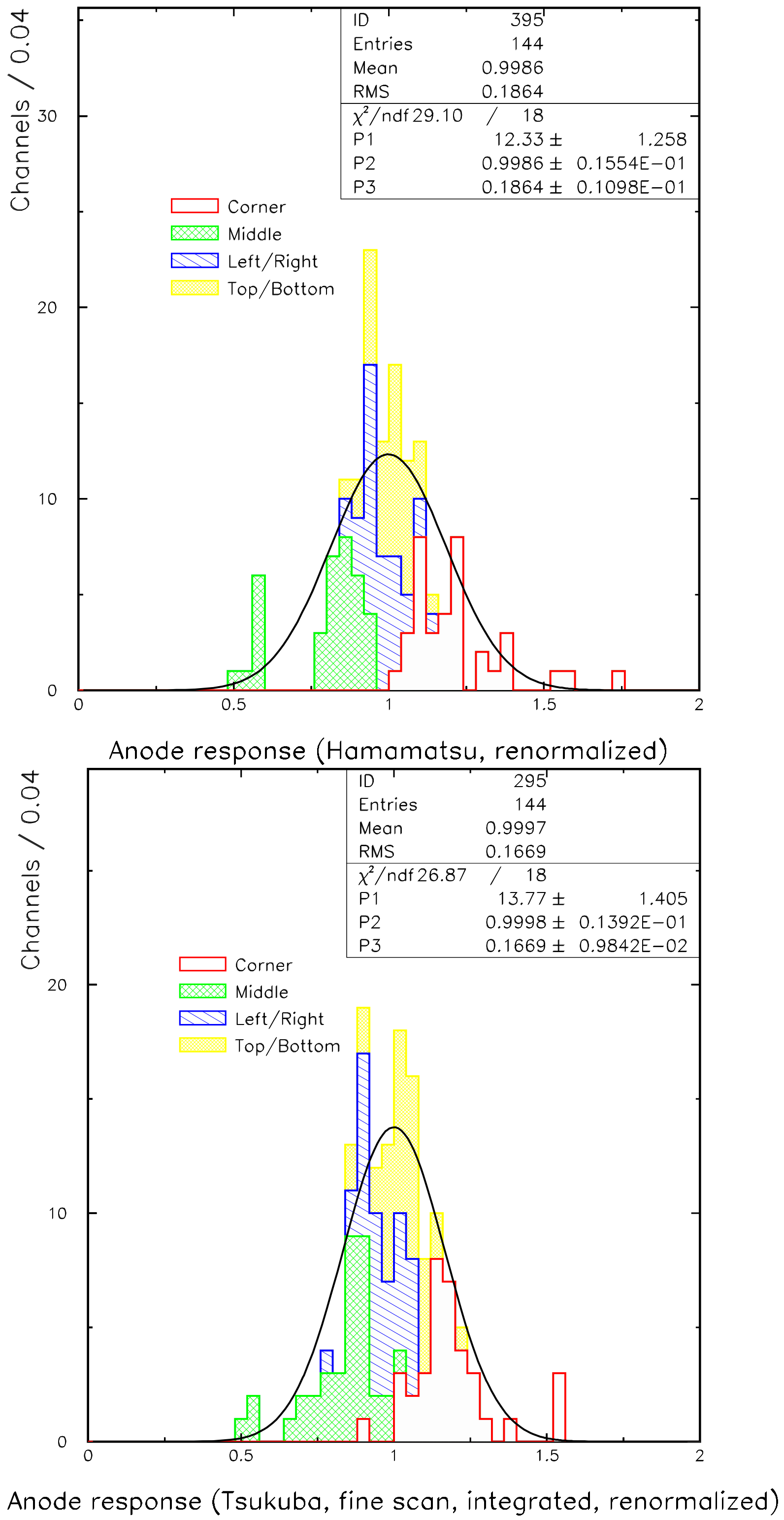

Figure 16: Distribution of re-normalized anode responses, as measured by Hamamatsu (full illumination) and at Tsukuba (fine scan, integrated).

ka2460 : 120502 : Front View

100	2.21 ±0.19	0.47 ±0.2	0.31 ±0.22
1.98 ±0.23	0.51 ±0.2	0.12 ±0.22	0.88 ±0.2
−0.02 ±0.21	0.16 ±0.2	0.57 ±0.21	0.22 ±0.22
0.11 ±0.2	−0.02 ±0.2	0.34 ±0.19	0.07 ±0.25

ch4

0.34 ±0.19	0.24 ±0.18	2.29 ±0.18	100
0 ±0.2	−0.09 ±0.19	0.64 ±0.2	2.81 ±0.19
0 ±0.2	0.09 ±0.18	0.59 ±0.19	0.42 ±0.19
−0.15 ±0.19	−0.25 ±0.19	0.26 ±0.2	−0.15 ±0.22

ch1

0.11 ±0.21	−0.07 ±0.19	−0.16 ±0.22	0 ±0.23
0.11 ±0.23	−0.09 ±0.19	0 ±0.24	−0.04 ±0.22
2.26 ±0.2	0.84 ±0.18	0.11 ±0.22	0.04 ±0.2
100	2.49 ±0.19	0.28 ±0.2	0.52 ±0.24

ch16

−0.06 ±0.17	0.23 ±0.19	0.31 ±0.18	−0.02 ±0.22
−0.02 ±0.21	−0.16 ±0.18	0.35 ±0.19	0.05 ±0.17
−0.11 ±0.2	0.31 ±0.17	0.38 ±0.19	2.55 ±0.17
−0.03 ±0.18	0.24 ±0.17	2.85 ±0.2	100

ch13

ka2460 : 120502 : Front View

0.9 ±0.25	2.72 ±0.21	0.84 ±0.23	0.12 ±0.26
2.57 ±0.26	100	2.62 ±0.24	0.55 ±0.23
0.41 ±0.22	2.25 ±0.24	0.78 ±0.24	0.39 ±0.23
0.1 ±0.22	0.17 ±0.23	0.1 ±0.21	−0.09 ±0.24

ch7

0.44 ±0.2	0.47 ±0.2	2.22 ±0.21	0.81 ±0.25
0.1 ±0.2	1.95 ±0.19	100	2.12 ±0.2
−0.2 ±0.21	0.38 ±0.19	2.34 ±0.22	−0.13 ±0.19
0.17 ±0.2	−0.05 ±0.2	0.13 ±0.21	0.23 ±0.24

ch6

0.15 ±0.23	0.07 ±0.23	0.16 ±0.25	−0.06 ±0.28
0.62 ±0.28	2.85 ±0.25	0.43 ±0.26	0 ±0.25
2.45 ±0.24	100	2.89 ±0.26	0.05 ±0.24
0.62 ±0.24	2.32 ±0.22	0.37 ±0.26	0.61 ±0.25

ch11

0 ±0.18	0.05 ±0.19	0.35 ±0.21	0.14 ±0.2
−0.12 ±0.22	0.53 ±0.19	2.7 ±0.19	0.61 ±0.19
−0.01 ±0.2	2.36 ±0.18	100	2.19 ±0.2
0.16 ±0.18	0.43 ±0.19	2.42 ±0.21	0.27 ±0.2

ch10

ka2460 : 120502 : Front View

3.71 ±0.2	0.65 ±0.2	0.34 ±0.24	0.16 ±0.21
100	2.37 ±0.23	0.15 ±0.22	0.18 ±0.22
2.05 ±0.21	0.54 ±0.22	0.25 ±0.23	0.2 ±0.21
0.35 ±0.22	−0.36 ±0.21	0.03 ±0.21	0.08 ±0.24

ch8

0.79 ±0.18	0.4 ±0.19	0.46 ±0.17	2.81 ±0.19
0.32 ±0.2	0 ±0.19	2.23 ±0.19	100
−0.19 ±0.18	−0.01 ±0.17	0.47 ±0.19	2.68 ±0.19
0.09 ±0.19	0.03 ±0.18	−0.05 ±0.19	0.12 ±0.2

ch5

0.18 ±0.28	0.07 ±0.24	0.47 ±0.28	0.36 ±0.28
3.12 ±0.27	0.45 ±0.27	0.22 ±0.28	0.48 ±0.28
100	2.19 ±0.25	−0.03 ±0.28	0.22 ±0.27
2.99 ±0.29	0.55 ±0.26	0.21 ±0.25	0.24 ±0.28

ch12

0.45 ±0.18	−0.01 ±0.18	0.53 ±0.21	0 ±0.19
0.12 ±0.2	−0.09 ±0.2	0.75 ±0.21	2.7 ±0.17
0.39 ±0.19	0.51 ±0.17	2.41 ±0.21	100
0.04 ±0.19	−0.13 ±0.18	0.43 ±0.2	3.3 ±0.21

ch9

ka2460 : 120502 : Front View

3.04 ±0.21	100	2.31 ±0.24	0.45 ±0.22
0.69 ±0.24	2.01 ±0.21	0.62 ±0.21	0.36 ±0.21
−0.32 ±0.2	−0.14 ±0.2	0.02 ±0.21	0.17 ±0.22
−0.13 ±0.2	−0.27 ±0.21	−0.06 ±0.23	0.16 ±0.24

ch3

0.47 ±0.17	2.86 ±0.2	100	2.79 ±0.21
0.36 ±0.21	0.52 ±0.21	2.34 ±0.2	0.52 ±0.2
0.09 ±0.2	0.25 ±0.19	−0.18 ±0.2	0.51 ±0.19
−0.11 ±0.2	−0.03 ±0.2	0.33 ±0.21	0.18 ±0.21

ch2

0.06 ±0.19	−0.2 ±0.18	0.02 ±0.21	0.16 ±0.22
0.26 ±0.23	0.34 ±0.2	0.05 ±0.23	0.34 ±0.2
0.91 ±0.19	2.32 ±0.18	0.72 ±0.22	−0.07 ±0.19
3.01 ±0.21	100	3.46 ±0.19	0.57 ±0.23

ch15

−0.12 ±0.2	0 ±0.18	−0.27 ±0.21	0.27 ±0.22
0.04 ±0.22	−0.1 ±0.21	0.2 ±0.22	0.21 ±0.21
0.27 ±0.2	0.39 ±0.18	2.13 ±0.21	0.2 ±0.19
0.41 ±0.18	3.45 ±0.2	100	2.64 ±0.23

ch14

Figure 17: Measurement of cross talks. The tube is illuminated with a 0.83-mm diameter fiber from a distance of 1 - 2 mm above the surface of the tube and at the center of the channels (ones with a response of 100).

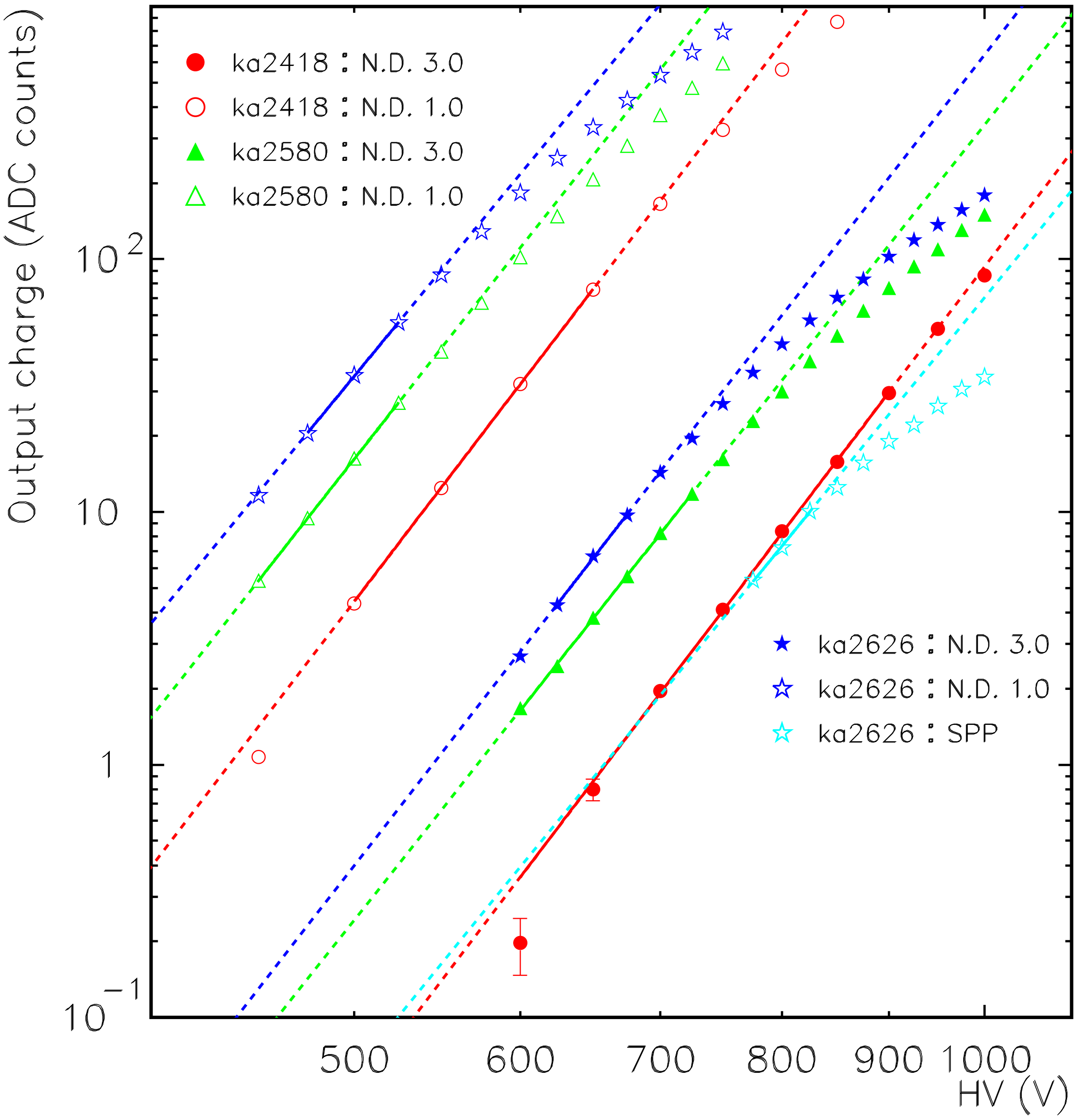

Figure 18: Measured pulse heights as a function of the applied high voltage value. Results of two kinds of tubes are shown, KA2580 and KA2626 (H6568, normal base) and KA2418 (H6568-10, tapered base). Two sets of measurements with different amounts of light are shown, intended to produce roughly 10 photoelectrons (N.D. 3.0) and 1000 photoelectrons (N.D. 1.0). For KA2626, single photoelectron measurements are shown as well.

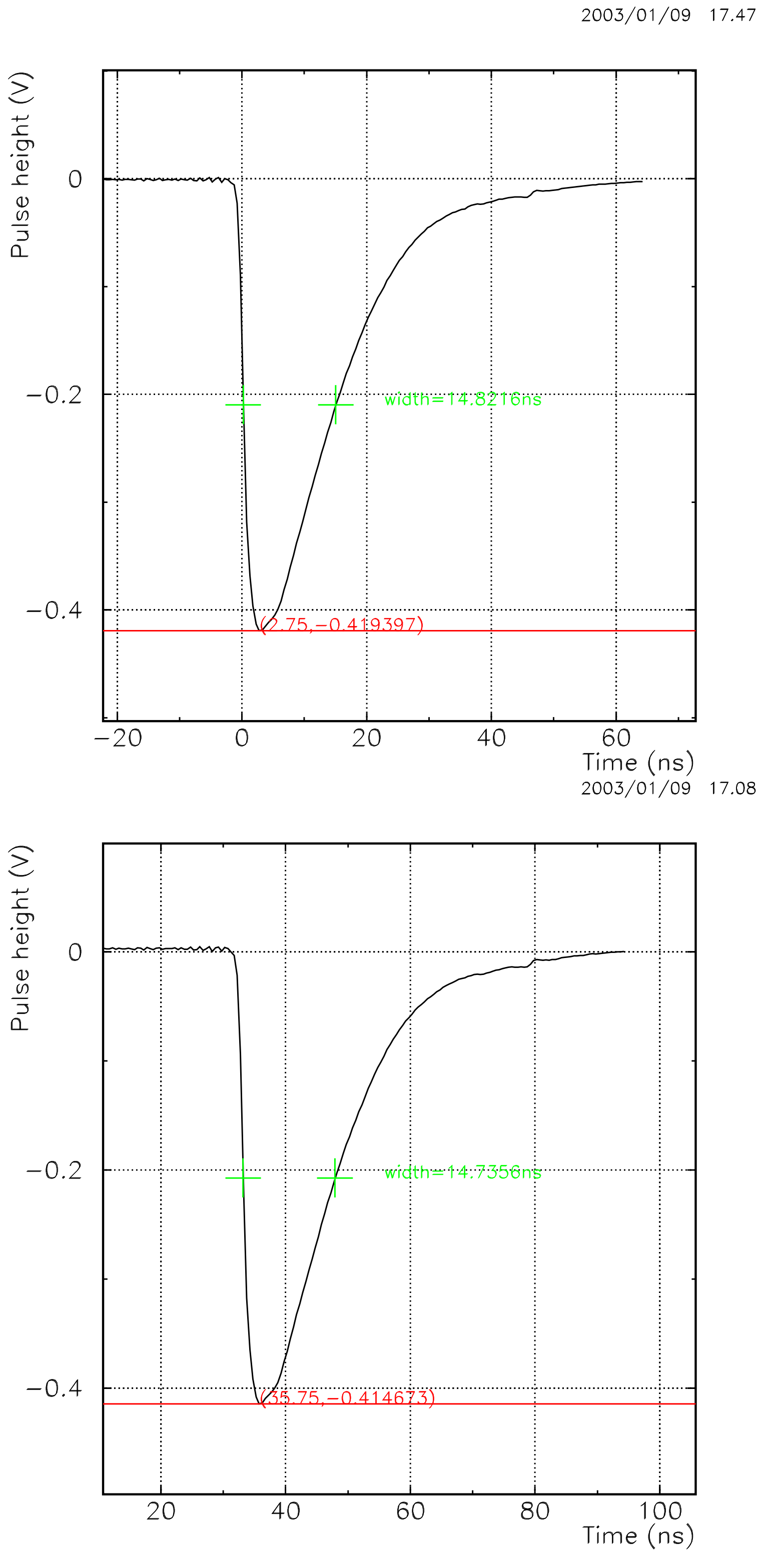

Figure 19: Oscilloscope pictures of average pulse shapes of tube KA2626 for light of roughly 1000 photoelectrons. Top: self-triggered. Bottom: triggered by laser. Tube voltage is at −700 V.

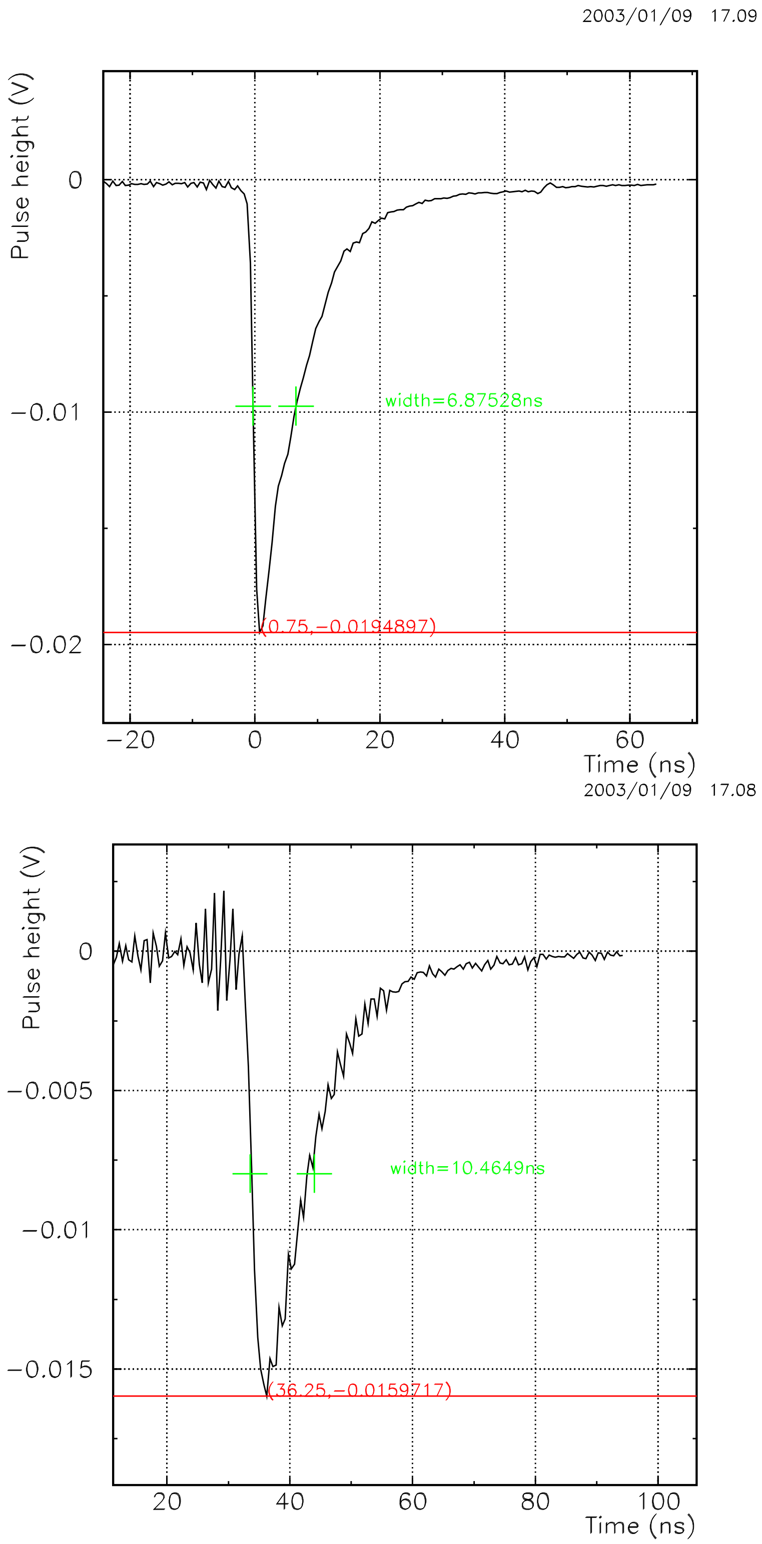

Figure 20: Oscilloscope pictures of average pulse shapes of tube KA2626 for light of roughly 10 photoelectrons. Top: self-triggered. Bottom: triggered by laser. Tube voltage is at −700 V.

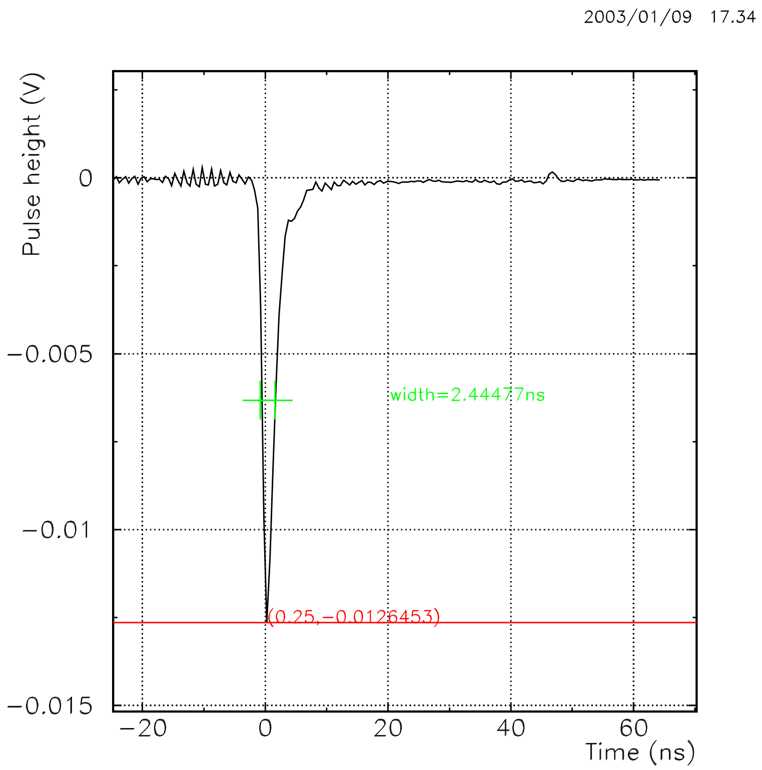

Figure 21: Oscilloscope pictures of average pulse shapes of tube KA2626 for single photoelectrons. Self-triggered. Tube voltage is at −700 V.

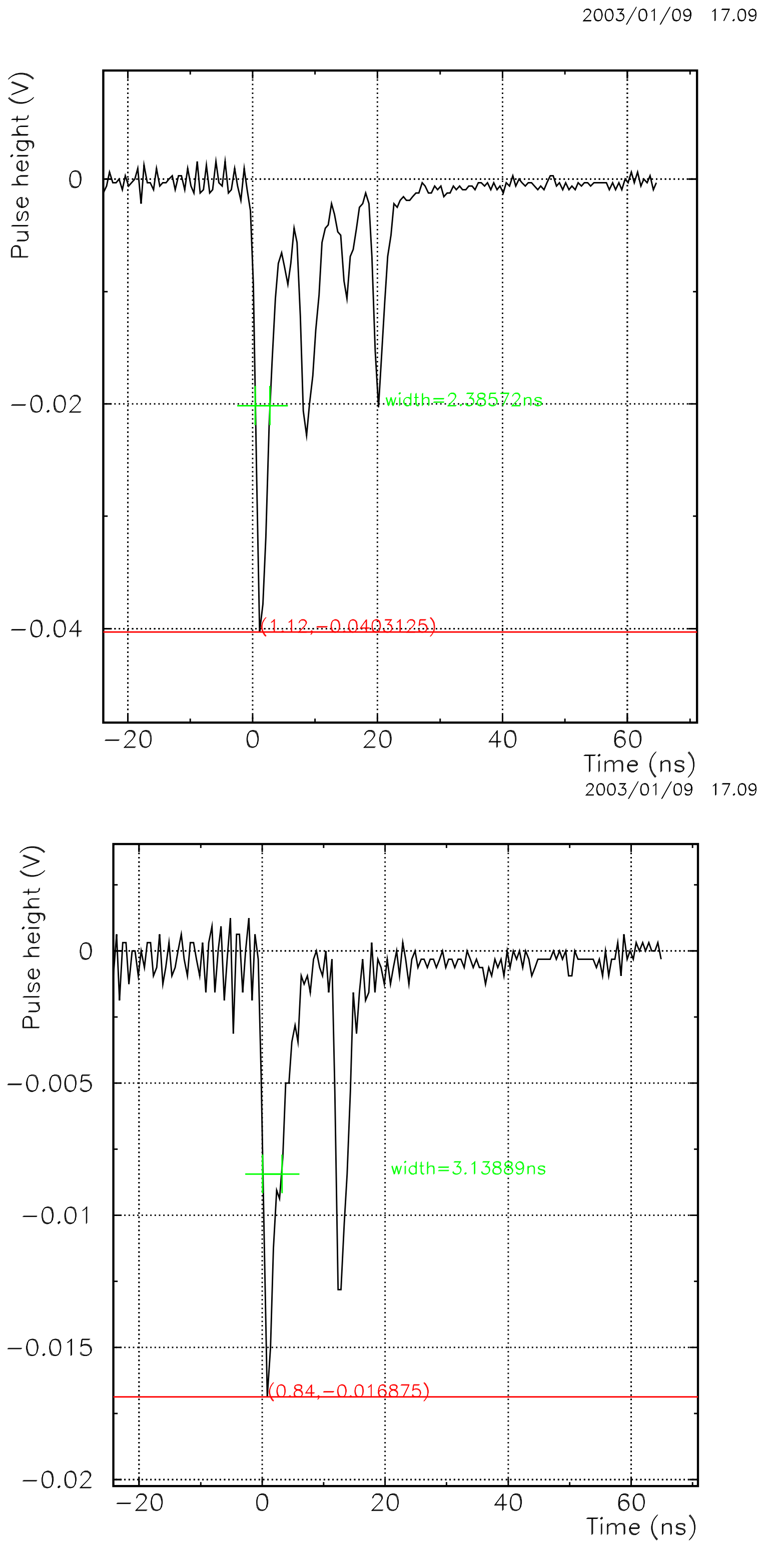

Figure 22: Oscilloscope pictures of single-shot pulse shapes of tube KA2626 for light of roughly 10 photoelectrons. Top: one event. Bottom: another event. Tube voltage is at −700 V.

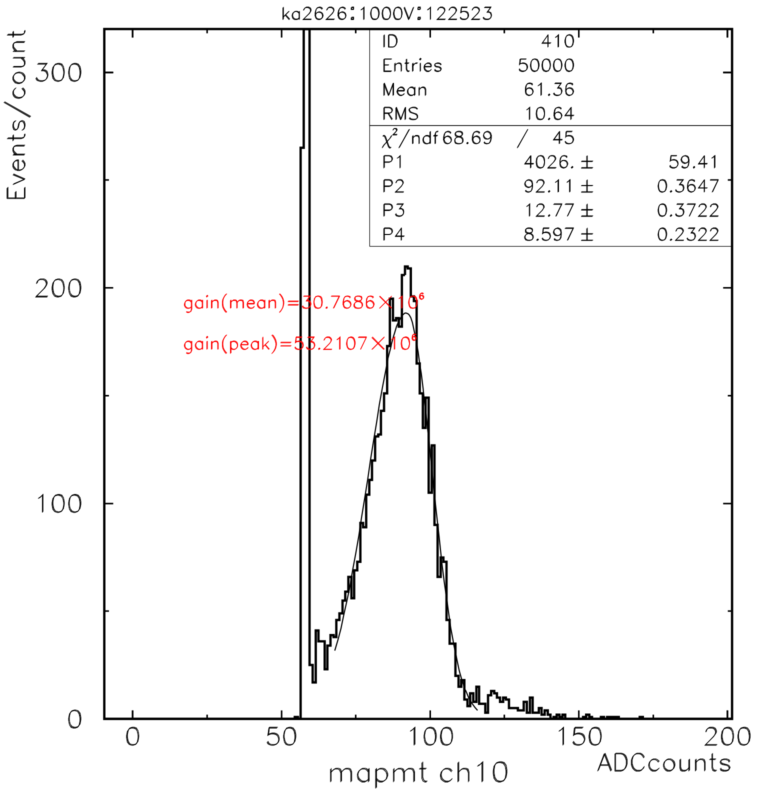

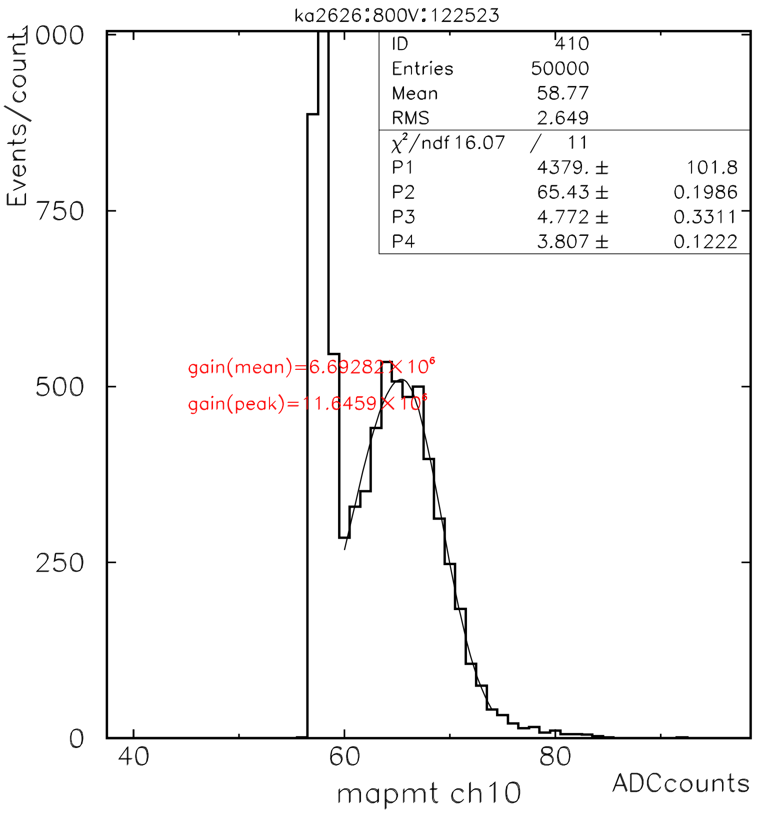

Figure 23: Pulse height distributions with very low amount of light (N.D. 4.5, roughly 0.3 photoelectrons), at high voltage of −1000 V (top) and −800 V (bottom). Tube KA2626, Channel 10.

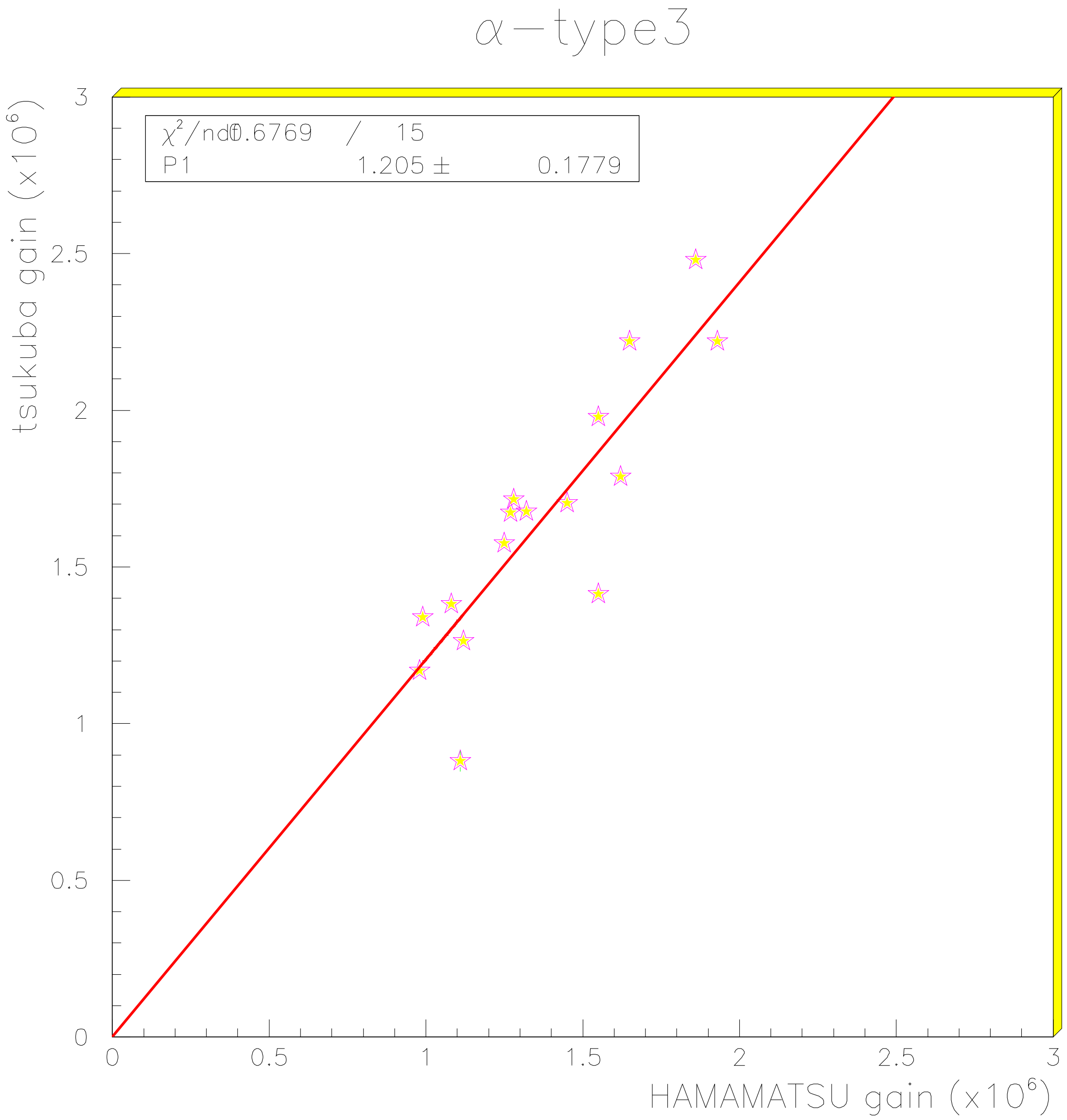

Figure 24: Comparison of absolute gains measured at Tsukuba from single photoelectron peaks to Hamamatsu data sheet values.

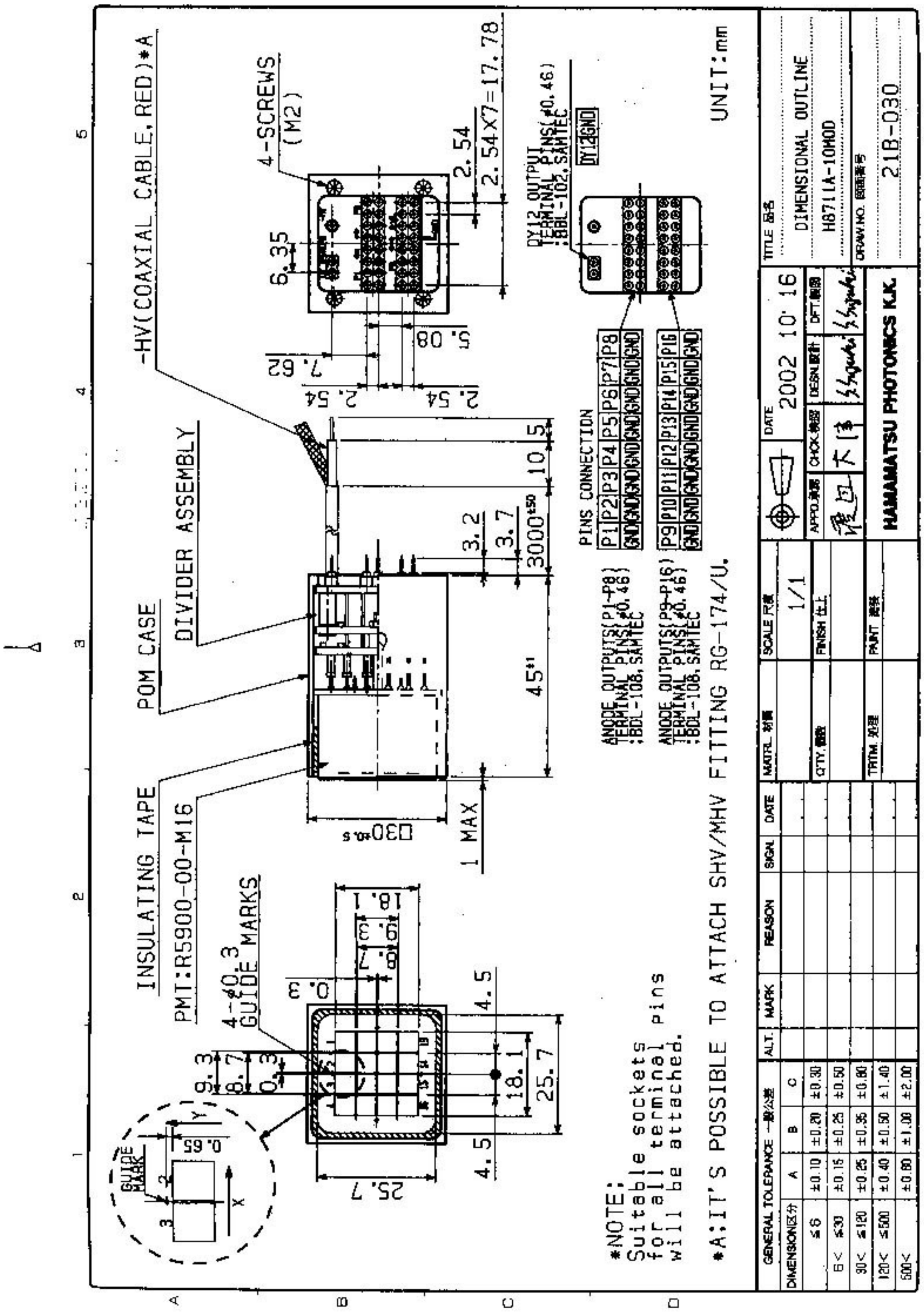

Figure 25: Mechanical drawing of the model H8711A-10MOD (by Hamamatsu).

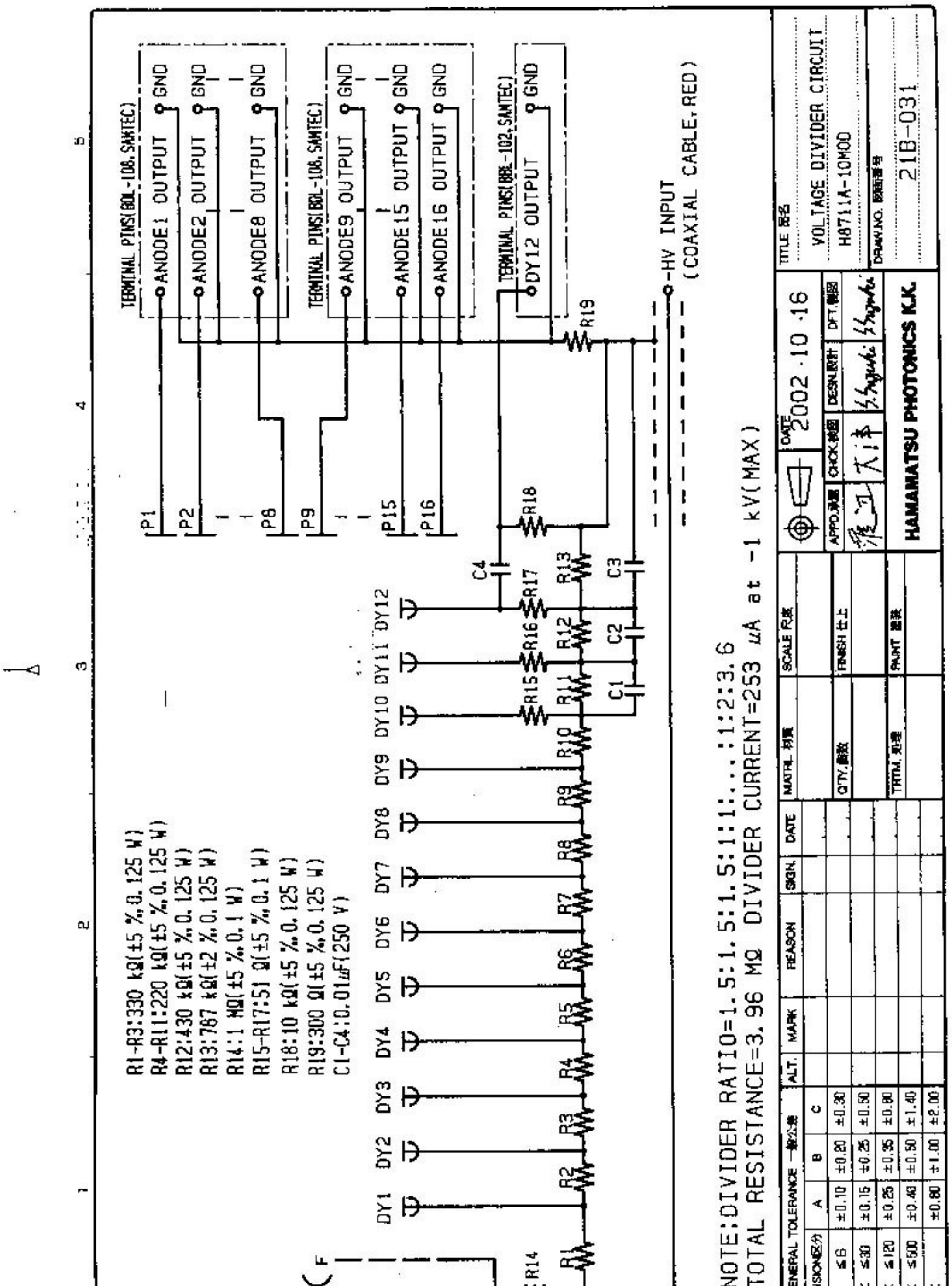

Figure 26: Electrical drawing of the model H8711A-10MOD (by Hamamatsu).